

# PREDICTING THE EFFECT OF CLIMATE CHANGE ON WILDFIRE SEVERITY AND OUTCOMES IN CALIFORNIA: PRELIMINARY ANALYSIS

*A Report From:*

**California Climate Change Center**

*Prepared By:*

**Jeremy S. Fried, USDA Forest Service  
Pacific Northwest Research Station, Forest Inventory  
and Analysis**

**J. Keith Gilles  
University of California, Berkeley  
Agricultural and Resource Economics**

**William J. Riley  
Lawrence Berkeley National Laboratory  
Center for Isotope Geochemistry**

**Tadashi J. Moody  
University of California, Berkeley  
Environmental Science, Policy, and Management**

**Clara Simon de Blas  
Universidad Rey Juan Carlos**

**Katharine Hayhoe  
ATMOS Research and Consulting**

**Max Moritz  
University of California, Berkeley  
Environmental Science, Policy, and Management**

**Scott Stephens  
University of California, Berkeley  
Environmental Science, Policy, and Management**

**Margaret Torn  
Lawrence Berkeley National Laboratory  
Center for Isotope Geochemistry**

## DISCLAIMER

This report was prepared as the result of work sponsored by the California Energy Commission (Energy Commission) and the California Environmental Protection Agency (Cal/EPA). It does not necessarily represent the views of the Energy Commission, Cal/EPA, their employees, or the State of California. The Energy Commission, Cal/EPA, the State of California, their employees, contractors, and subcontractors make no warrant, express or implied, and assume no legal liability for the information in this report; nor does any party represent that the uses of this information will not infringe upon privately owned rights. This report has not been approved or disapproved by the California Energy Commission or Cal/EPA, nor has the California Energy Commission or Cal/EPA passed upon the accuracy or adequacy of the information in this report.



Arnold Schwarzenegger, *Governor*

WHITE PAPER

March 2006  
CEC-500-2005-196-SF

## Preface

The Public Interest Energy Research (PIER) Program supports public interest energy research and development that will help improve the quality of life in California by bringing environmentally safe, affordable, and reliable energy services and products to the marketplace.

The PIER Program, managed by the California Energy Commission (Energy Commission), annually awards up to \$62 million to conduct the most promising public interest energy research by partnering with Research, Development, and Demonstration (RD&D) organizations, including individuals, businesses, utilities, and public or private research institutions.

PIER funding efforts are focused on the following RD&D program areas:

- Buildings End-Use Energy Efficiency
- Energy-Related Environmental Research
- Energy Systems Integration
- Environmentally Preferred Advanced Generation
- Industrial/Agricultural/Water End-Use Energy Efficiency
- Renewable Energy Technologies

**The California Climate Change Center (CCCC)** is sponsored by the PIER program and coordinated by its Energy-Related Environmental Research area. The Center is managed by the California Energy Commission, Scripps Institution of Oceanography at the University of California at San Diego, and the University of California at Berkeley. The Scripps Institution of Oceanography conducts and administers research on climate change detection, analysis, and modeling; and the University of California at Berkeley conducts and administers research on economic analyses and policy issues. The Center also supports the Global Climate Change Grant Program, which offers competitive solicitations for climate research.

**The California Climate Change Center Report Series** details ongoing Center-sponsored research. As interim project results, these reports receive minimal editing, and the information contained in these reports may change; authors should be contacted for the most recent project results. By providing ready access to this timely research, the Center seeks to inform the public and expand dissemination of climate change information; thereby leveraging collaborative efforts and increasing the benefits of this research to California's citizens, environment, and economy.

For more information on the PIER Program, please visit the Energy Commission's website [www.energy.ca.gov/pier/](http://www.energy.ca.gov/pier/) or contact the Energy Commission at (916) 654-5164.

# Table of Contents

Preface.....	ii
Executive Summary .....	1
1.0 Introduction.....	2
2.0 Methods .....	3
2.1. The Study Area: CDF's Amador-El Dorado Unit.....	3
2.2. Climate Forcing .....	6
2.3. Fire Behavior .....	8
2.4. Initial Attack Simulation .....	9
3.0 Results.....	11
3.1. Climate.....	11
3.2. Fire Behavior .....	27
3.3. Initial Attack Simulation .....	32
4.0 Conclusions .....	42
5.0 References.....	46

## List of Figures

Figure 1. Mean 2 p.m. temperature for the high and transition fire seasons, for the location of the Bald Mountain weather station, for BASE, MIDCEN, and ENDCEN, by scenario.....	13
Figure 2. Mean 2 p.m. relative humidity for the high and transition fire seasons, for the location of the Bald Mountain weather station, for BASE, MIDCEN, and ENDCEN, by scenario....	14
Figure 3. Number of very dry days (relative humidity < 15%) for the high and transition fire seasons, for the location of the Bald Mountain weather station, for BASE, MIDCEN, and ENDCEN, by scenario .....	15
Figure 4. Average daily precipitation for the high and transition fire seasons, for the location of the Bald Mountain weather station, for BASE, MIDCEN, and ENDCEN, by scenario .....	18
Figure 5. Precipitation intensity for the high and transition fire seasons, for the location of the Bald Mountain weather station, for BASE, MIDCEN, and ENDCEN, by scenario.....	19
Figure 6. Annual number of wet days for the high and transition fire seasons, for the location of the Bald Mountain weather station, for BASE, MIDCEN, and ENDCEN, by scenario .....	20
Figure 7. Average 10-hour fuel moisture (percent) for the high and transition fire seasons, for the location of the Bald Mountain weather station, for BASE, MIDCEN, and ENDCEN, by scenario.....	23
Figure 8. Wind direction for the high and transition fire seasons, for the location of the Bald Mountain weather station, for BASE, MIDCEN, and ENDCEN, by scenario.....	24
Figure 9. Average wind speed for the high and transition fire seasons, for the location of the Bald Mountain weather station, for BASE, MIDCEN, and ENDCEN, by scenario.....	25
Figure 10. Annual number of very windy days (wind speed > 15 mph) for the high and transition fire seasons, for the location of the Bald Mountain weather station, for BASE, MIDCEN, and ENDCEN, by scenario.....	26
Figure 11. Mean annual escapes, by Fire Management Analysis Zone, for base, mid-century, and end-of-century periods modeled by GFDL for the A2 (high GHG) scenario.....	40
Figure 12. Mean annual escapes, by Fire Management Analysis Zone, for base, mid-century, and end-of-century periods modeled by GFDL for the B1 (reduced GHG) scenario .....	41

## List of Tables

Table 1. Fuel combinations for the Amador-El Dorado Unit.....	5
Table 2. Predicted temperature, humidity, and fuel moisture for the Amador-El Dorado Unit.	12
Table 3. Predicted precipitation for the Amador-El Dorado Unit.....	17
Table 4. Predicted wind for the Amador-El Dorado Unit.....	22
Table 5. Mean rates of spread (chains per hour) for the high fire season (June 15–October 15) for selected fuel-weather station-slope class-period combinations under climate model GFDL2.1, scenario A2 .....	28
Table 6. Mean rates of spread (chains per hour) for the high fire season (June 15–October 15) for the 95th percentile values for selected fuel-weather station-slope class combinations under climate model GFDL2.1, scenario A2 .....	29
Table 7. Mean rates of spread (chains per hour) for the high fire season (June 15–October 15) for selected fuel-weather station-slope class-period combinations under climate model GFDL2.1, scenario B1.....	30
Table 8. Mean rates of spread (chains per hour) for the high fire season (June 15–October 15) for the 95th percentile values for selected fuel-weather station-slope class combinations under climate model GFDL2.1, scenario B1.....	31
Table 9. Historical (1990 to 2000) and GFDL (BASE) Scenario A2 escapes, ESL fires, and area burned by contained fires for the main fuel types in the Amador El Dorado Unit.....	33
Table 10. CFES2 predictions for the GFDL GCM and both climate scenarios .....	34
Table 11. CFES2 predictions for the GFDL GCM and both climate scenarios. ....	36
Table 12. CFES2 predictions for the PCM GCM and both climate scenarios .....	37
Table 13. GFDL, scenario A2, 90th and 95th percentile number of ESL fires per year .....	38
Table 14. Effect of adding a CDF engine at the El Dorado Hills station post-climate change under GFDL-A2.....	39

## **Executive Summary**

This white paper focuses on how climate change-induced effects on weather will translate into changes in wildland fire severity and outcomes, particularly on the effectiveness of initial attack at limiting the area burned in contained fires and the number of fires that escape initial attack. Prior research has indicated that there is a potential for significant increases in the number of fires escaping initial attack, particularly in areas in which the fuel matrix is dominated by grass and brush. These results were driven primarily by predicted increases in wind speeds. Those findings, however, were derived using less sophisticated models of initial attack than currently available.

The results of this study, using more sophisticated models and climate projections, indicate that subtle shifts in fire behavior of the sort that might be induced by the climate changes anticipated for the next century are of sufficient magnitude to generate an appreciable increase in the number of fires that escape initial attack, at least for areas where brush fuels dominate. Such escapes of considerable importance in wildland fire protection planning, given the high cost to society of a catastrophic escape like those experienced in recent decades in the Berkeley-Oakland, Santa Barbara, San Diego, or Los Angeles areas. However, at least for the limited region in the Sierra Nevada considered in this study, it would appear that relatively modest augmentations to existing firefighting resources would be sufficient to compensate for change-induced changes in wildland fire outcomes.

Generalizing our findings with respect to wildland fire intensity and outcomes for the Amador-El Dorado Unit to other private lands in the state will require both further analysis using the data for that CDF unit, and replication of this analysis using data for several other units and for the state's federal forest lands.

No attempt is made in this paper to extrapolate the results beyond the boundaries of the study area, in part because of necessary work that was identified with respect to further validation of this study's modeling approach.

## 1.0 Introduction

Previous analyses of wildfire and climate change suggested that wildfire outcomes (the number of escaped fires and area burned annually) would increase, sometimes dramatically, in northern California under a double-CO<sub>2</sub> scenario (Fried et al. 2004; Torn and Fried 1992). In one extension of limited results to all nonfederal lands in this region, a double-CO<sub>2</sub> climate was predicted to lead to a doubling in the frequency of fires that escape initial attack suppression, thereby potentially becoming large, damaging fires (Fried et al. 2004). Others have commented that given the importance of extreme fire weather in California, it is critical that we better understand how this weather is impacted by climate change (Davis and Michaelsen 1995). These results raise several important follow-on questions: Will climate change lead to changes in the number of fires (i.e., to fire occurrence), changes in the beginning and end dates of fire season for which fire agencies must be fully staffed, or shifts in fire rate-of-spread distributions? Can additional firefighting resources compensate for increased fire severity or occurrence? At what cost? Would lower greenhouse gas (GHG) emissions pathways moderate the projected impacts on wildfire relative to a higher emissions scenario? This white paper attempts to address some of these questions. Although much more work remains to be done to address them completely, this preliminary analysis indicates that existing models can be extended in ways that provide valuable insights into the impact of climatic change on wildfire severity and outcomes in California over the next century.

The results reported in this paper differ from prior studies in that they were derived by using a more sophisticated initial attack simulator and higher resolution climate scenarios than were previously available. Unfortunately, time constraints limited our analysis to a consideration of a single representative northern California administrative unit of the California Department of Forestry and Fire Protection (CDF)—Amador-El Dorado (AEU). (Note: Most CDF units are one- or two-county administrative area). In prior work (Fried et al. 2004), AEU presented the highest sensitivity to climate change of the three units considered. Preliminary estimates for the effects of climate change on wildfire severity and outcomes for AEU are presented below for higher and lower emission scenarios: business-as-usual and reduced-anthropogenic-emission scenarios.

## **2.0 Methods**

This study relied on models and data drawn from California's strategic fire planning system to estimate aspects of climate change relevant to wildland fire at three levels of analysis. The first level focused on generating 150 years of simulated daily weather variables from 1950 to 2099 that relate to fire behavior via downscaling from general circulation model simulations under two GHG emissions scenarios for three periods: a baseline reference period from 1961 to 1999 denoted henceforth as BASE; a second period in the middle of this century (2035 to 2064) denoted as MIDCEN; and a third period at the end of the century (2070 to 2099) denoted as ENDCEN. In the second level of analysis, these predictions of daily weather were used, in turn, to predict the wildfire behavior attributes rate of spread (ROS) and burning index (BI) by using the Fire Behavior Dispatch Modeling System (FBDMOD) (CDF 1992), a program patterned after the National Fire Danger Rating System (Deeming et al. 1977). Fire behavior predictions were made for a wide range of fuel and slope conditions in the study area, both to explore how these attributes would respond to climate change, and to generate inputs for the third level of analysis. In the third level of analysis, this study sought to assess the impact of these predicted changes on the success of the initial attack system that forms the foundation of wildland fire protection in California. Individual wildfire outcomes were predicted and then aggregated by using the California Fire Economics Simulator version 2 (CFES2) (Fried and Gilless 1999), a stochastic computer model developed for the California Department of Forestry and Fire's (CDF) fire protection planning program. This section describes the detailed methods and assumptions for each level of analysis, and how the models and data from each level were ultimately combined to predict wildfire outcomes under alternative climate change scenarios.

### **2.1. The Study Area: CDF's Amador-El Dorado Unit**

All analysis reported in this paper relates to our pilot study area: CDF's Amador-El Dorado Unit, which encompasses the area in the Sierra foothills east of Sacramento in Amador and El Dorado counties where the CDF has primary responsibility for wildfire suppression, with assistance from cooperating local and federal agencies. The AEU covers 0.9 million hectares (2 million acres) and contains a range of vegetation types from annual grasslands, shrublands, oak savannas, and open pine woodlands in the west, to short- and long-needled coniferous forests in the east, reflecting the effects of elevation and rainfall gradients. Census data from [www.CensusScope.org](http://www.CensusScope.org) show that the AEU experienced population growth in excess of the state average during the 1990s, increasing the value of infrastructure at risk and increasing the complexity of the problems faced there by local, state, and federal fire protection agencies.

For purposes of strategic and tactical planning, CDF conducts analysis by using the Fire Protection Planning System. The agency stratified this unit into nine fire management analysis zones (FMAZs) that are described by a combination of fuel type (e.g., grass, brush—an indicator of the fire regime) and population density (as an indicator of the extent to which issues of wildland urban interface are germane). For modeling fire potential within a FMAZ, CDF relies on representative fire locations (RFLs) chosen on the basis of historical fire locations, each of which is characterized by a particular fire behavior fuel model, slope class, herbaceous vegetation type, climate class, and most representative fire weather station (for the conditions at the RFL). We conceive of these concatenated weather and behavior attribute labels as “fuel combinations.” Each FMAZ is considered homogenous with respect to some of these variables

(weather station, climate class and herb class) but specific fuel model and slope class are allowed to differ among RFLs within a FMAZ.

Fuel models used in AEU (A, B, C, F, H, and U) are from the National Fire Danger Rating System (narrative descriptions can be found in Deeming et al., 1977). Percentage slope, a key value in predicting fire behavior, is classed 1 (0% to 25%) through 5 (> 75%). Herbaceous vegetation, which has varying effects on fire behavior depending on fuel type and can be classified as either annual (A) or perennial (P), is classified as annual throughout this unit. Because of the Mediterranean climate, characterized by cold, wet winters and warm, dry summers, climate class is coded as 2 (subhumid, savanna). Fire weather stations used for fire behavior prediction in AEU are located at Bald Mountain (lat 38 54 3, long 120 41 8) and Georgetown (lat 38 55 10, long 120 54 0). Table 1 lists the specific fuel combinations used to represent fire behavior in AEU.

The structure of the Fire Protection Planning System guides the analysis undertaken for this study at all three levels. Daily weather is modeled for the locations of the two representative fire weather stations for level 1. Predicted weather for those locations and the fuel combinations that occur on the unit are used to model fire rate of spread in a level 2 analysis. And for level 3, fire behavior results are combined with information on the existing initial attack organization to predict initial attack success.

**Table 1. Fuel combinations for the Amador-EI Dorado Unit**

<b>Fuel model</b>	<b>Description</b>	<b>Slope class (percent)</b>	<b>Herb class</b>	<b>Climate class</b>	<b>Associated weather station</b>
A1	Grassland	0–25	Annual	2	Bald Mountain
A1	Grassland	26–40	Annual	2	Bald Mountain
B1	Brush	26–40	Annual	2	Bald Mountain
B1	Brush	41–55	Annual	2	Bald Mountain
B1	Brush	56–75	Annual	2	Bald Mountain
C1	Open pine	0–25	Annual	2	Bald Mountain
C1	Open pine	26–40	Annual	2	Bald Mountain
C1	Open pine	41–55	Annual	2	Bald Mountain
H1	Short-needle conifer	41–55	Annual	2	Bald Mountain
H1	Short-needle conifer	56–75	Annual	2	Bald Mountain
U1	Closed pine	0–25	Annual	2	Bald Mountain
U1	Closed pine	41–55	Annual	2	Bald Mountain
U1	Closed pine	56–75	Annual	2	Bald Mountain
A1	Grassland	26–40	Annual	2	Georgetown
B1	Brush	0–25	Annual	2	Georgetown
B1	Brush	26–40	Annual	2	Georgetown
B1	Brush	41–55	Annual	2	Georgetown
B1	Brush	56–75	Annual	2	Georgetown
C1	Open pine	0–25	Annual	2	Georgetown
C1	Open pine	26–40	Annual	2	Georgetown
C1	Open pine	41–55	Annual	2	Georgetown
C1	Open pine	56–75	Annual	2	Georgetown
F1	Brush–chamise	41–55	Annual	2	Georgetown

## 2.2. Climate Forcing

Projections of fire weather under future climate change scenarios are based on temperature and precipitation from simulations of BASE and future periods (MIDCEN and ENDCEN) for two atmosphere-ocean general circulation models (AOGCMs): the NOAA-GFDL CM2.1 (Delworth et al. 2005), denoted henceforth as *GFDL*; and the DOE-NCAR Parallel Climate Model (Washington et al. 2000), denoted as *PCM*. Simulations are forced by the *IPCC Special Report on Emission Scenarios* mid-high (A2) and lower (B1) emissions scenarios (SRES, Nakićenović et al. 2000). The A2 scenario describes a very heterogeneous world where economic development is regionally oriented, economic growth and technological change occurs relatively slowly, and emissions climb steeply, reaching 30 gigatons of carbon per year (GtC/yr) or 6 times 1990 levels, by 2100. In contrast, emissions under the B1 scenario are lower, based on a world that transitions relatively rapidly to service and information economies. The CO<sub>2</sub> emissions in the B1 scenario peak at just below 10 GtC/yr—around two times 1990 levels—at mid-century and decline slowly to below current-day levels. Although both scenarios are “nonintervention” (i.e., do not include any specific actions to reduce emissions), the lower emissions under the B1 scenario can be taken as a proxy to compare with A2 to evaluate the potential benefits of following a lower versus a higher emissions pathway.

The GFDL and PCM monthly temperature and precipitation fields for the A2 and B1 scenarios were then statistically downscaled to daily values for regions with a resolution of 1/8°, or about 12 kilometers (km) (7 miles) (Wood et al. 2002), each covering one of the two fire weather stations of interest in Alameda and El Dorado Counties. Downscaling used an empirical statistical technique that maps the probability density functions for modeled monthly and daily precipitation and temperature for the climatological period (1961 to 1990) onto those of gridded historical observed data, so the mean and variability of both monthly and daily observations are reproduced by the climate model data. The bias correction and spatial disaggregation technique is one originally developed for adjusting AOGCM output for long-range streamflow forecasting (Wood et al. 2002), later adapted for use in studies examining the hydrologic impacts of climate change (VanRheenen et al. 2004), and compares favorably to other statistical and dynamic downscaling techniques (Wood et al. 2004). The Variable Infiltration Capacity (VIC) distributed land surface hydrology model was then used to generate daily average relative humidity values that correspond to the daily temperature and precipitation for each grid cell.

Daily maximum temperature, minimum temperature, precipitation, and humidity are only four of the variables required as inputs to FBDMOD. Thus, observed weather data for each fire station was next used in conjunction with the modeled variables to project daily 2 p.m. temperature and relative humidity, precipitation duration, maximum and minimum relative humidity, 10-hour fuel moisture, wind direction and speed, and state of the weather for all periods, as follows:

**Wind Direction.** A statistical CART (classification and regression tree) algorithm was used to first resolve the wind “seasons” for each station as defined by statistically significant differences in average distributions. Most of the 15 stations had only two distinctly different seasons, but several had three or four. For each station and season, a second CART analysis was then performed to identify the primary characteristics of the weather system identified with each wind direction, in terms of humidity, temperature, diurnal temperature range, and precipitation. Based on the weather characteristics

associated with specific wind directions, probability distributions of wind direction were created for various weather types. Daily model data was then classified by season and weather type, and the wind direction for that day sampled from the appropriate distribution.

**Wind Speed.** For each station and “wind season” identified above, a probability distribution of wind speed for each of the eight wind directions was created from historical observed data. Daily modeled wind speed was then determined by first obtaining the wind direction for the day based on the weather state characteristics (as described above), then sampling from the distribution of wind speeds corresponding to that wind direction for that season in order to produce a reasonable distribution of wind speeds that reflected both the projected change in daily conditions as well as the actual wind speeds that had been observed at that station over the historical period.

**Maximum and Minimum Relative Humidity.** As the climate and hydrology models only simulate daily average humidity, it was also necessary to parameterize maximum and minimum daily values. Using the observed fire weather data for each station, this study first assessed the degree to which a range of temperature and average humidity variables were correlated with the daily range in relative humidity. For all stations, diurnal temperature range (dT) was found to be most strongly correlated with the difference between *average* and *minimum* relative humidity. Based on the observed records for each station, the difference between average and minimum relative humidity was then grouped into categories (binned) based on the diurnal temperature range. Modeled dT was calculated and the appropriate bin sampled from to determine the  $RH_{avg} - RH_{min}$  difference. Values for  $RH_{max}$  and  $RH_{min}$  were then determined from simulated  $RH_{avg}$ .

**2 p.m. Temperature and Humidity.** Representative values of temperature and relative humidity at 2 p.m., to reflect the time of day required for representing worst-of-the-day fire behavior in FBDMOD, were developed by first determining which other variables in the observed data were most strongly correlated with 2 p.m. temperature and humidity. These were found to be maximum daily temperature and minimum daily relative humidity. The observed correlation between observed  $T_{max}$  and  $T_{2pm}$ , and between  $RH_{min}$  and  $RH_{2pm}$  was then used to bin the *difference* between observed 2 p.m. data values and  $T_{max}$  and  $RH_{min}$  data. Based on modeled  $T_{max}$  and  $RH_{min}$  values, the corresponding bin was selected and the modeled daily 2 p.m. values determined through random sampling from the appropriate distribution based on observed differences.

**Precipitation Duration.** Average duration of precipitation during the day was set to zero if total precipitation amount was zero. For precipitation amounts greater than zero, 12 monthly bins were created for a total of 144 bins based on observed weather at individual stations, with daily precipitation amounts for each bin ranging from 1 through 20 in increments of 5, then up to a maximum value. Observed duration of precipitation was binned by month and by daily total to create historical distributions of the probability of precipitation duration by station and month. These distributions were then randomly sampled for modeled precipitation to determine representative precipitation duration values for each day of the corresponding month.

**State of the Weather.** The daily weather state is a complex function of season, temperature, precipitation, cloudiness, humidity, and numerous other variables not directly simulated by the modeled data used here. In lieu of direct information on weather states, the category for each day was determined based on a number of modeled variables, including the ratio of total precipitation to duration (differentiating between rain, showers, or drizzle), maximum humidity and minimum temperature (to determine the likelihood of fog), maximum temperature below 2°C (36°F) and precipitation (to identify snow or sleet events), high lightning probability combined with nonzero precipitation (for thunderstorms), and the diurnal temperature range (to identify the likely presence or absence of clouds, the presence of which would moderate both daily high and nighttime low temperatures).

**10-Hour Fuel Moisture.** The relationships between observed values of 10-hour fuel moisture (10-hr FM) and a number of other climate variables were examined. It was determined that the strongest correlation was with daily average relative humidity, temperature, and precipitation, without a significant time lag. An empirical formula for 10-hr FM was determined based on the observed values such that 10-hr FM was parameterized as a function of relative humidity divided by temperature with a flag for nonzero precipitation. Simulated values of RH, T, and precipitation were then used to calculate 10-hr FM for each day.

As described above, detailed daily fire weather projections have been sampled from actual observed weather conditions specific to each station based on simulated daily maximum and minimum temperatures, relative humidity, and precipitation as calculated by two AOGCMs and downscaled to a high-resolution grid cell centered over that station. As such, they are expected to produce statistically similar (although not identical) fire behavior patterns over the historical period and realistically represent the effect of projected changes on fire behavior under future scenarios of climate change at specific fire weather stations.

### **2.3. Fire Behavior**

Daily fire rate of spread and burning index (a proxy for intensity) was predicted for the three periods (BASE, MIDCEN, and ENDCEN) for each fuel combination present in AEU under the higher (A2) and lower emissions (B1) scenarios as simulated by the GFDL and PCM models and transformations described in the previous section as input to FBDMOD. A key assumption in these fire behavior predictions is that they represent fires that spread at near daily worst-case rates, without crowning or spotting, through continuous fuels on a uniform slope (NWCG 2002). Weather station descriptive information required by FBDMOD (elevation, latitude, date of vegetation green-up, date of first killing frost) was obtained from the publicly available fire weather archives of the National Fire and Aviation Management Web (<http://famweb.nwcg.gov/weatherfirecd/index.htm>).

The fire behavior algorithms contained in FBDMOD allow for the option of calculating 10-hour fuel moistures endogenously by FBDMOD. We chose to calculate 10-hour fuel moistures exogenously from our GCM weather streams instead, as these values produced generally more conservative estimates of fire behavior. FBDMOD also requires the user to estimate when herbaceous plant growth begins and when plants first freeze in the fall (i.e., green-up and frost dates). We applied a January 1 green-up date and December 31 frost date to all years of the

study so as to minimize the impact of these unknown parameters on fire behavior for two reasons: historical evidence as to what these dates should be was lacking, and dynamically estimating green-up and frost dates annually based on other weather variables was beyond the scope of this analysis. Using these dates may have caused slight underestimation of potential fire behavior in the winter and early spring months (particularly for grass-driven fuel models).

This study compared changes in fire behavior predictions between periods by using Tukey's Honestly Significant Difference (HSD) test for multiple comparisons, a method based on the range of the sample means. Neither students-t test nor analysis of variance (ANOVA) are suitable for this data because the values of ROS and BI for a given period are not distributed normally. The Tukey HSD test does not mandate assumptions of normality or equal variances. Also, when comparing the period means for the levels of the factor time in an analysis of variance, simple comparisons using t-tests would inflate the probability of declaring a significant difference when one is not, in fact, present. When comparing samples of unequal sizes (such as our data), the Tukey HSD test is conservative. We compared means calculated for the portions of the ROS distributions modeled as beta distributions in CFES2 (leaving out only the slowest moving fires); we also compared means of the highest 5% of the values in each ROS distribution to explore potential increases in "extreme" fire weather.

#### **2.4. Initial Attack Simulation**

The event-based simulation framework of CFES2 allows users to evaluate initial attack response effectiveness for a given unit. This model simulates realistic fires and suppression responses through the use of stochastic modules for fire occurrence and fire behavior (Gilles and Fried 1999; Fried and Gilles 1988), and lists of fire suppression resources with their response times and fireline production rates. For a given simulated season, CFES2 simulates fire events with specific locations and start dates and times, and estimates the behavior (rate of spread or burning index) of these fires by drawing from distributions of potential fire behavior (beta and Bernoulli) for a specific fuel combination and season. This study used daily fire behavior predictions generated with FBDMOD to generate the distributions of potential fire behavior necessary for CFES2 analysis.

Daily-resolved fire behavior predictions were divided into five inter-annual seasons for CFES2 analysis by using FORTRAN for data manipulation: low 1 (January 1 to May 15), transition 1 (May 15 to June 15), high (June 15 to October 15), transition 2 (October 15 to November 15) and low 2 (November 15 to December 31). These seasons are used in CFES2 to specify what fire suppression resources are available, and have previously been estimated based on fire occurrence (Gilles and Fried 1999). An important question when studying fire and climate change is how the high fire season might change in timing and extent. Although it is likely that fire suppression agencies would alter management techniques to accommodate a changing climate, we held these dates constant throughout our studies under a "ceteris paribus" approach (i.e., "all other things being equal"). This forces the assumption that although potential fire behavior intensity might change for a particular time of year, the firefighting resources available would not.

Separate distributions of potential fire behavior were modeled for the low, transition, and high fire seasons. Fire behavior data for a particular season is consistently bimodal in its distribution, with a large number of slow moving fires coupled with a wider distribution of fast-moving fires

(Fried and Gilless 1988). Each overall seasonal distribution was thus split into two smaller distributions, and fit with Bernoulli (slow-moving fires) and beta (fast-moving fires) curves. Determining both where to split the data and the best fitting curves for the resulting data was accomplished through iterations of a chi-square test and the moments method of curve fitting in the statistical program R. Distribution parameters were summarized for input into CFES2.

These fire behavior indices served as inputs to CFES2, along with additional detailed input data from CDF on, for example, the locations and productivity of fire suppression resources, and historical fire ignition patterns. CFES2 was then used to generate estimates of the frequency of escaped fires and the area burned by contained fires, and to evaluate the effectiveness of alternative configurations and levels of initial attack resources. Simulations were conducted for the BASE, MIDCEN, and ENDCEN periods, for the A2 and B1 scenarios, by using behavior data generated from both the GFDL and PCM AOGCMs, with 200 “years” (actually, realizations of years) simulated for each scenario.

When using CFES2 to conduct comparative analysis, any of a number of kinds of results can prove interesting, including changes in the frequency of escapes, area burned in contained fires by season, size class, and geographical unit; percentage of fires that are successfully contained within predetermined size limits; and even utilization frequency and dispatching costs of any particular firefighting resource or group of resources. And, because CFES2 is a stochastic simulator that produces as many potential realizations as desired, we can look beyond a single, deterministic result for any attribute of interest, and report information on variability (e.g., standard errors) along with expected values, or even selected percentiles of the distribution of realizations (Fried et al. 2006). This analysis focused on estimates of the expected value (and standard errors) of escaped fires per year by FMAZ, and secondarily on the area burned by contained fires. The critical lessons to be learned are the extent to which these change with climate in a statistically significant fashion.

Important assumptions were made in our CFES2 simulations to make the analysis tractable. Somewhat tempering the definitiveness of these results, many parameters that may well change over the next century were held constant, including fire occurrence, fuel models, the amount, positioning, and productivity of firefighting resources, and population density.

## 3.0 Results

### 3.1. Climate

The impact of global climate change on daily weather characteristics at the location of the Bald Mountain weather station differs widely by variable. This section examines changes specifically in fire season weather (defined as bracketing the range from May 1 to November 30 of each year) for MIDCEN and ENDCEN relative to BASE. In some cases the projected changes are larger under a higher emissions scenario (A2 versus B1), illustrating the sensitivity of fire weather to emissions pathways and the degree of global change; in others, the GFDL model shows changes that are distinctly different from the PCM model, highlighting inter-model uncertainty; and in some cases, changes are not consistent either between models or scenarios, displaying a more random component that may be indicative of the sensitivity of that variable to multiple and interactive changes in and feedbacks between climate characteristics.

The 2 p.m. temperature displays the most robust changes, consistent across both models and scenarios (Table 2, Figure 1). By midcentury, a change of 1.1°F to 3.5°F (0.6°C to 1.9°C) is projected under B1 and 1.9°F to 4.2°F (1.1°C to 2.3°C) under A2. As expected, the inter-scenario difference grows by end-of-century where projected changes range from 2.4°F to 4.8°F (1.3°C to 2.7°C) (B1) up to 4.3°F to 8.5°F (2.4°C to 4.7°C) (A2). Larger changes are seen for GFDL, the more sensitive model, as compared to PCM. Under the higher A2 scenario, both GFDL and PCM exhibit significant changes in the standard deviation of the distribution that are not as evident under B1, with both A2 temperature distributions developing smaller peaks and longer tails over time. These changes in the shape of the distribution are indicative of more frequent extreme temperature events, particularly at the higher end of the range.

Relative humidity (RH) changes display a strong dependence on both the model and the emissions scenario (Table 2, Figure 2). The model determines the sign of the change, with GFDL being consistently drier and PCM more humid. However, the emissions scenario (higher or lower) tends to determine the magnitude of change for each model, with larger changes for A2 relative to B1. For 2 p.m. RH values, GFDL projects decreases ranging from -6% (B1) to -9% (A2) by MIDCEN and -5% (B1) to -13% (A2). In contrast, PCM simulations show small increases in average RH of +1% (B1) to +3% (A2) by MIDCEN and +3% (B1) or no change (A2) by ENDCEN. Focusing specifically on low-humidity days (defined as 2 p.m. RH less than 15%) intensifies the inter-model differences (Figure 3). The GFDL model shows increases in the number of low-humidity days, up from a total of 28 or 29 on average during each fire season for BASE to 34 days (B1) or 46 days (A2) on average for each fire season by ENDCEN. In contrast, PCM simulates 35 low-humidity days under BASE, and projects decreases in this number of -2 days (B1) to -11 days (A2) by ENDCEN.

**Table 2. Predicted temperature, humidity, and fuel moisture for the Amador-EI Dorado Unit**

	<u>MEAN</u>			<u>STANDARD DEVIATION</u>		
	BASE	MIDCEN	ENDCEN	BASE	MIDCEN	ENDCEN
<b>2 PM TEMPERATURE (°F)</b>						
GFDL A2	70.99	75.11	79.45	13.77	14.61	15.44
PCM A2	70.99	72.87	75.26	13.74	13.93	13.94
GFDL B1	70.82	74.35	75.64	13.89	14.48	14.50
PCM B1	71.02	72.16	73.42	13.78	14.03	13.91
<b>2 PM RELATIVE HUMIDITY (%)</b>						
GFDL A2	37.47	34.01	32.63	20.67	20.13	20.16
PCM A2	35.72	36.68	35.54	20.31	20.10	20.05
GFDL B1	37.47	35.27	35.78	20.67	20.18	20.52
PCM B1	36.13	36.50	37.38	20.51	20.18	20.08
<b>10-HR FUEL MOISTURE (%)</b>						
GFDL A2	9.43	9.47	9.49	7.01	7.21	7.07
PCM A2	9.45	9.35	9.43	7.11	6.91	7.04
GFDL B1	9.44	9.45	9.37	6.97	7.09	6.90
PCM B1	9.35	9.40	9.40	6.96	7.02	7.02
<b>LOW HUMIDITY DAYS (&lt; 15% 2 PM RELATIVE HUMIDITY)</b>						
GFDL A2	29.43	39.27	46.10			
PCM A2	35.13	28.00	33.00			
GFDL B1	28.43	34.10	33.60			
PCM B1	34.83	29.30	24.30			

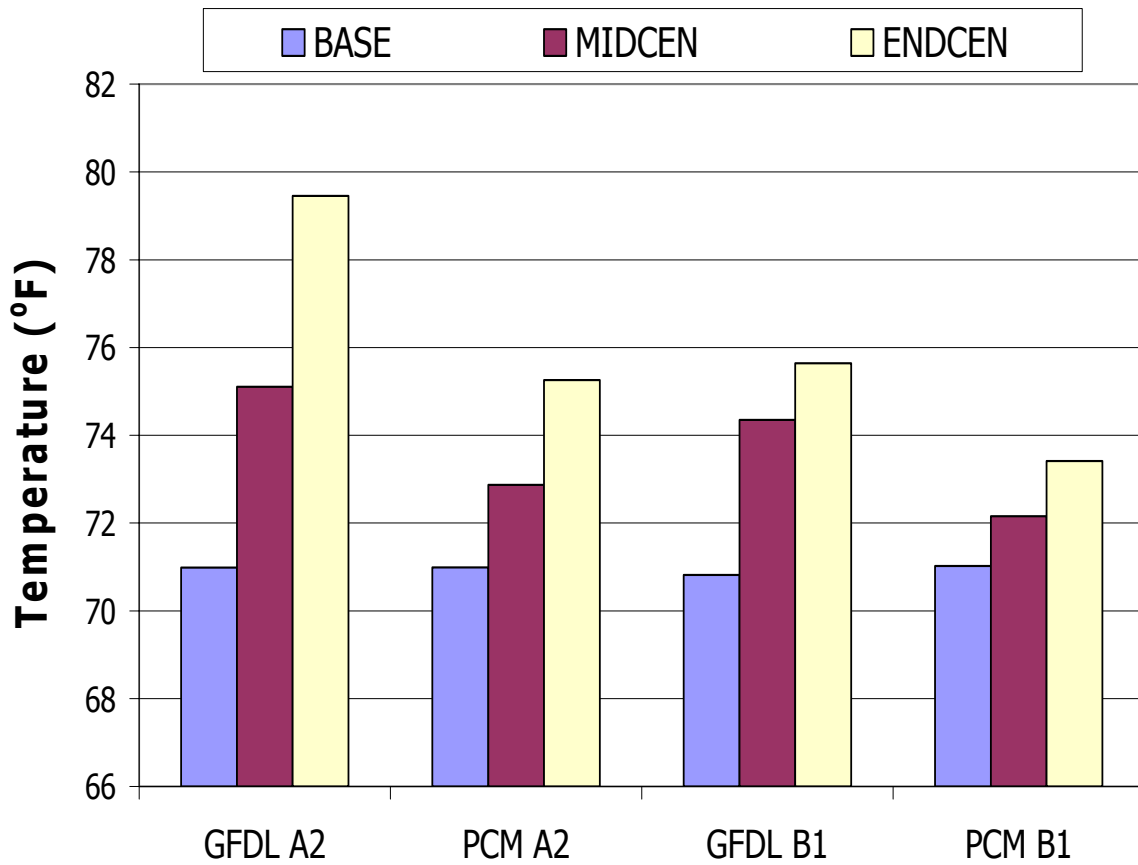


**Figure 1. Mean 2 p.m. temperature for the high and transition fire seasons, for the location of the Bald Mountain weather station, for BASE, MIDCEN, and ENDCEN, by scenario**

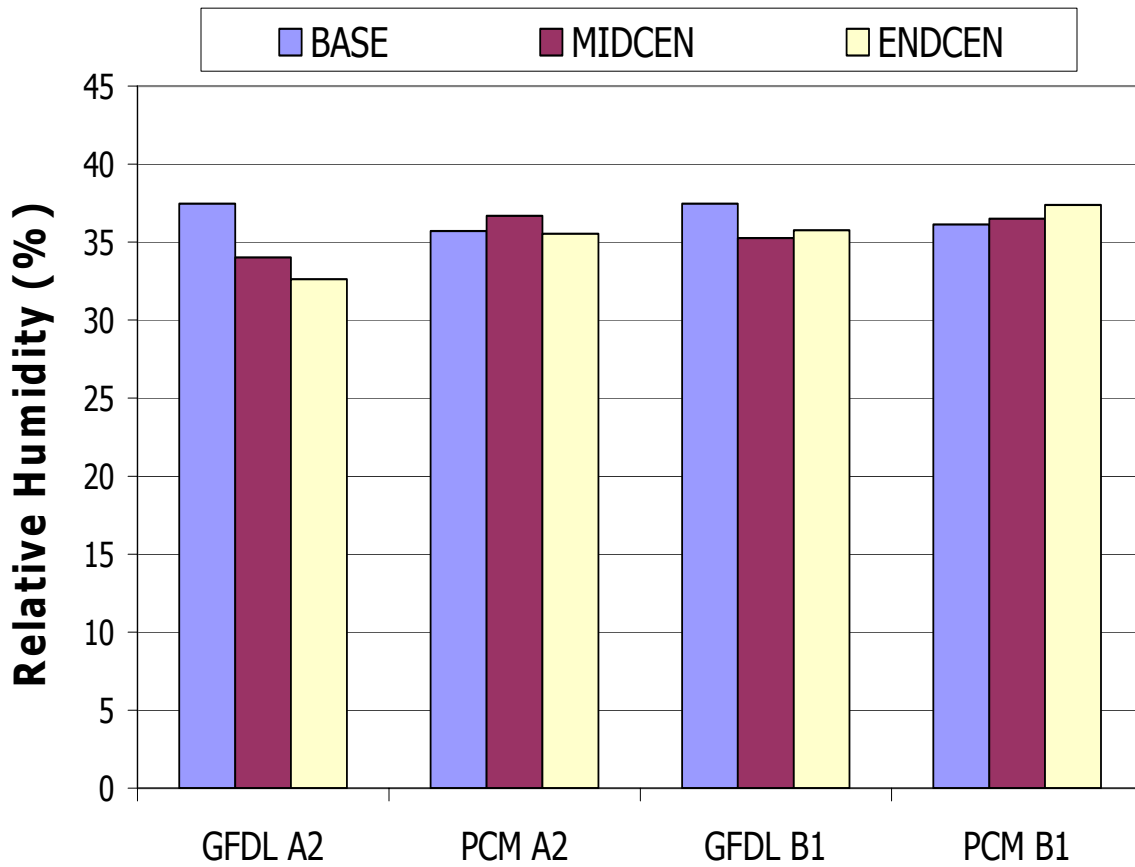


**Figure 2. Mean 2 p.m. relative humidity for the high and transition fire seasons, for the location of the Bald Mountain weather station, for BASE, MIDCEN, and ENDCEN, by scenario**

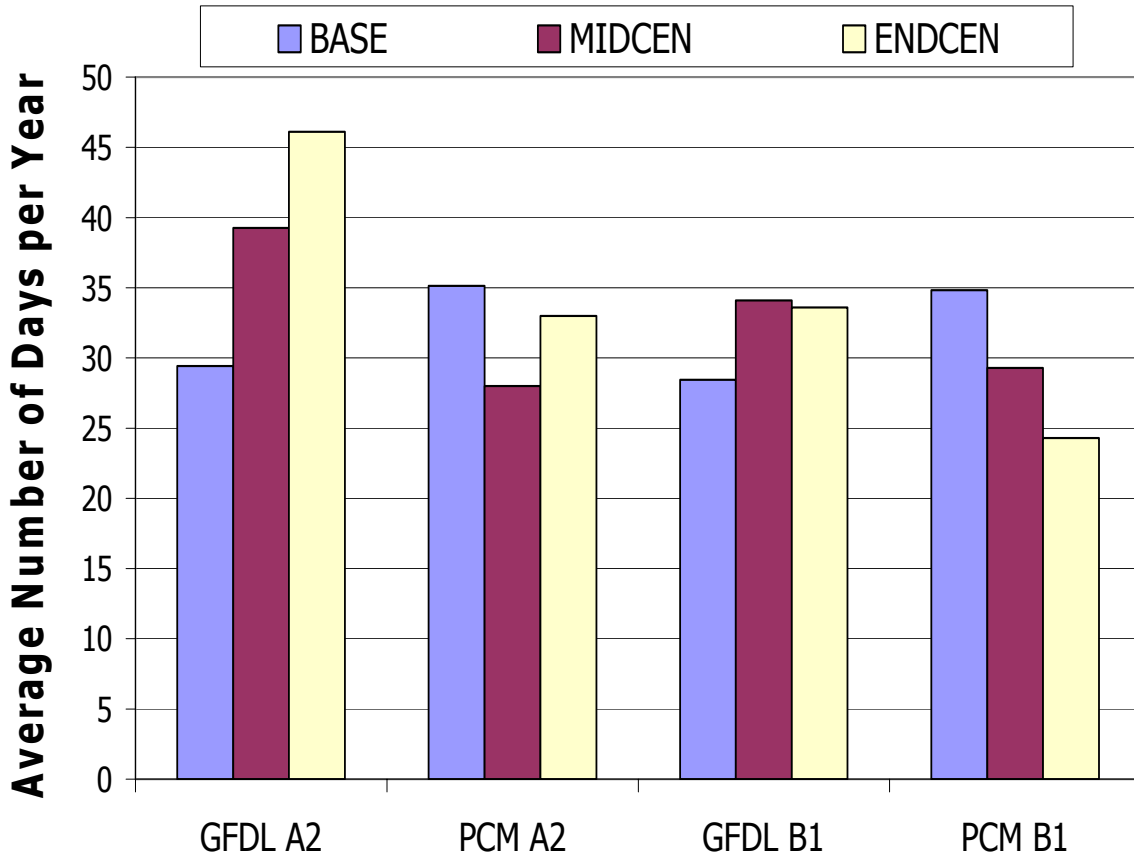


**Figure 3. Number of very dry days (relative humidity < 15%) for the high and transition fire seasons, for the location of the Bald Mountain weather station, for BASE, MIDCEN, and ENDCEN, by scenario**

Precipitation is similar to RH in that the sign of the change is determined by the model, but the magnitude is a function of the emissions scenario (larger changes for A2 relative to B1 for each model). However, although the models disagree in the sign of the change for MIDCEN (with GFDL showing decreases and PCM increases), by ENDCEN all model-scenario combinations suggest drier conditions (Table 3, Figure 4). For this location, the GFDL projects decreases in precipitation of 5% to 23% at MIDCEN and 13% to 34% at ENDCEN. The PCM shows increases on the order of 5% to 12% at MIDCEN, but at ENDCEN, a very small decrease (< 1%) is seen for B1 and a decrease of -8% for A2. Projected changes in the *intensity* of precipitation (measured as the total precipitation for the fire season divided by the number of wet days), display the same model-scenario split for MIDCEN, with GFDL projecting less intense precipitation and PCM more (Table 3, Figure 5). However, at ENDCEN all models and scenarios are in agreement that the intensity of precipitation will decrease. This is indicative of either less rain or more wet days or both, with overall less rain falling on a given wet day. Decreases range from -16% to -20% for GFDL and -8% for both PCM scenarios. Direct calculations of the number of wet days illustrate how intensity is a strong influence as at ENDCEN, all but the GFDL A2 simulation show more wet days per season (Figure 6). The GFDL A2 scenario shows fewer wet days (-8 days) but also much less precipitation (-34%), producing a net decrease in intensity despite the decrease in actual number of wet days.

**Table 3. Predicted precipitation for the Amador-El Dorado Unit**

	<u>MEAN</u>			<u>STANDARD DEVIATION</u>		
	BASE	MIDCEN	ENDCEN	BASE	MIDCEN	ENDCEN
<b>PRECIPITATION (AVERAGE PER DAY, IN HUNDREDTHS OF INCHES)</b>						
GFDL A2	6.92	5.33	4.59	64.65	58.59	54.94
PCM A2	6.20	6.91	5.70	67.42	65.99	61.94
GFDL B1	6.92	6.56	6.03	61.85	67.13	62.95
PCM B1	6.20	6.51	6.19	60.52	60.63	54.42
<b>NUMBER OF WET DAYS PER YEAR</b>						
GFDL A2	46.40	42.87	38.37			
PCM A2	44.87	44.27	44.90			
GFDL B1	45.37	43.90	47.23			
PCM B1	43.90	44.53	47.53			
<b>PRECIPITATION INTENSITY (ANNUAL TOTAL/NUMBER OF RAINY DAYS)</b>						
GFDL A2	31.89	26.59	25.61			
PCM A2	29.57	33.42	27.17			
GFDL B1	32.62	31.96	27.31			
PCM B1	30.22	31.30	27.89			

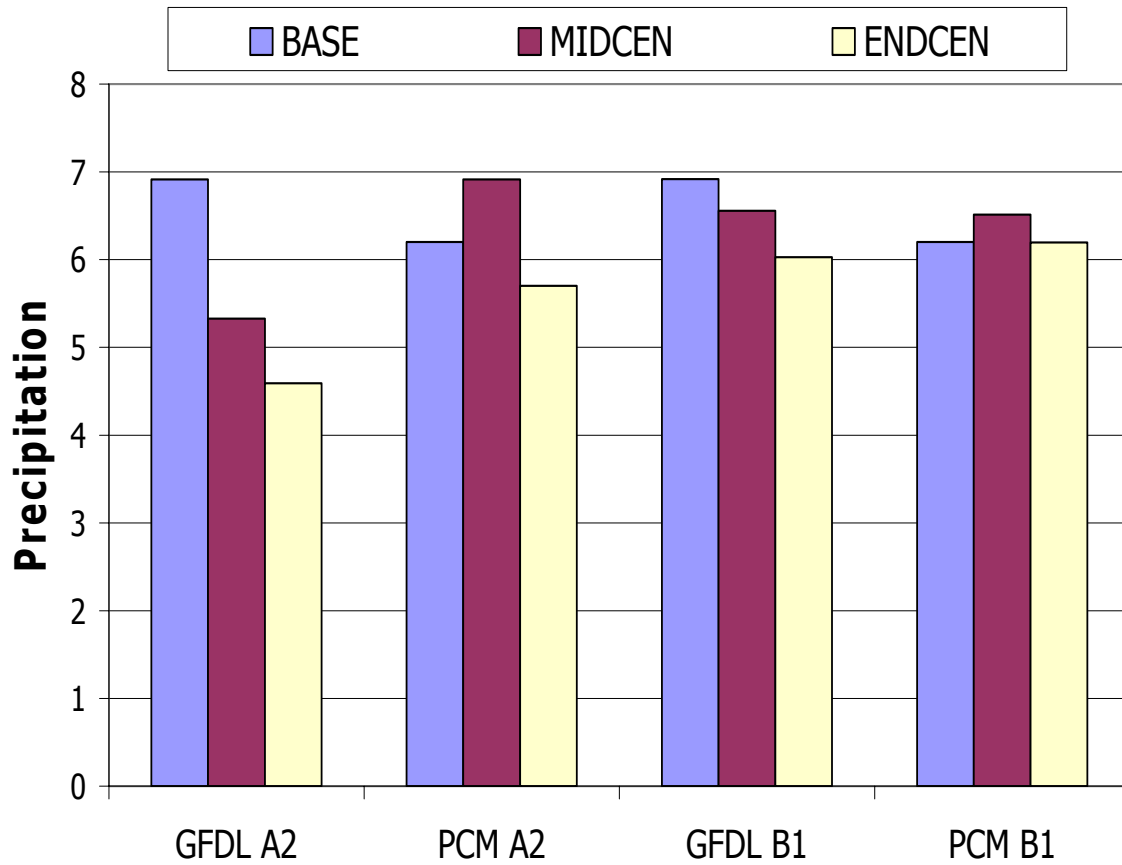


**Figure 4. Average daily precipitation for the high and transition fire seasons, for the location of the Bald Mountain weather station, for BASE, MIDCEN, and ENDCEN, by scenario**

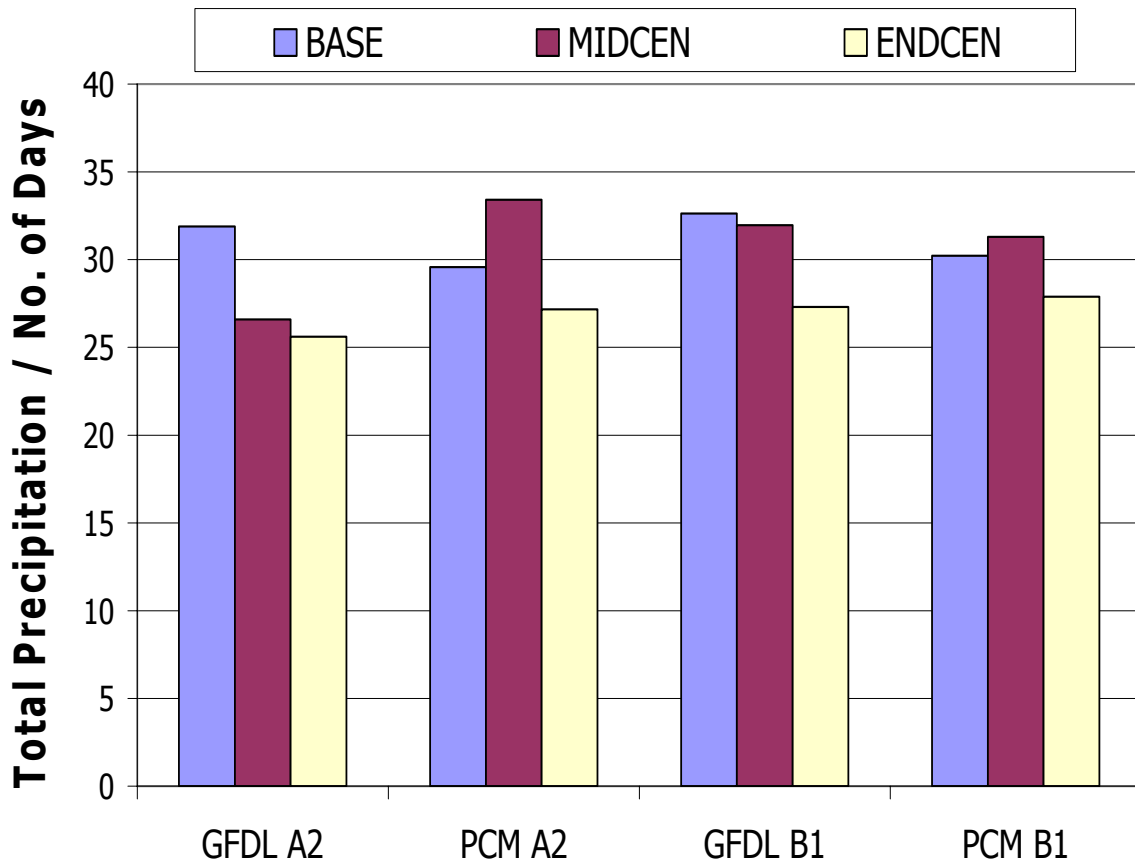


**Figure 5. Precipitation intensity for the high and transition fire seasons, for the location of the Bald Mountain weather station, for BASE, MIDCEN, and ENDCEN, by scenario**

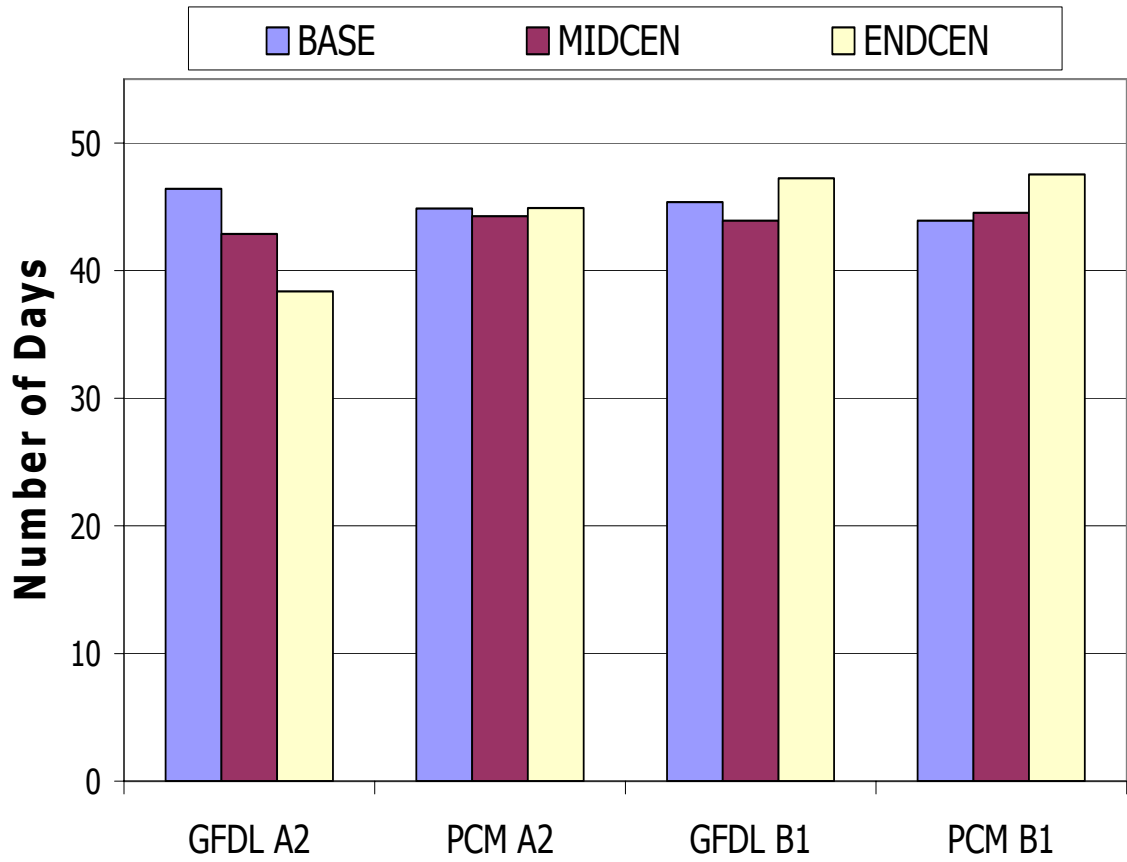


**Figure 6. Annual number of wet days for the high and transition fire seasons, for the location of the Bald Mountain weather station, for BASE, MIDCEN, and ENDCEN, by scenario**

The 10-hr FM is parameterized as proportional to relative humidity and precipitation and inversely proportional to temperature. As we have already seen how temperature increases consistently across all model-scenario combinations while the sign of RH and precipitation changes tend to be determined by each model, FM is a good example of a variable where projected changes are likely to be inconsistent across models and scenarios owing to its sensitivity to multiple climate characteristics that may not be changing in consistent ways. We would not expect to see consistent changes in projected future FM values, and this is in fact exactly what we do see (Table 2, Figure 7). At ENDCCEN, GFDL A2 and PCM B1 simulations show tiny increases of 1%. Although GFDL A2 has a large increase in temperature and a small decrease in humidity, which would act to reduce FM, the projected large increase in precipitation (+34%) at ENDCCEN wins out, producing very slightly higher FM values for GFDL A2 relative to BASE. In contrast, PCM B1 has a smaller increase in temperature, which, coupled with a small increase in humidity and no change in precipitation, also results in a 1% increase in average FM. The PCM A2 scenario shows no change at all, whereas GFDL B1 has a decrease of -1%, again owing to the confounding factors of a small temperature increase, RH decrease, and precipitation increase.

Wind is a function of both direction and speed. For almost all future periods and model-scenario combinations (the sole exception being PCM B1 ENDCCEN), simulations project an average fire season wind direction of 4 to 5 on a north-initiated, clockwise 8-point directional scale (S/SE) that shifts upward, indicating a seasonal average change in wind direction toward the south and west (Table 4, Figure 8). This could be indicative of increasing land-sea temperature gradients and hence more offshore winds. Changes in wind speed are extremely inconsistent, displaying no uniform dependence on either model or scenario. At MIDCCEN, GFDL projects very small increases in average wind speed from 0.3% (B1) to 0.6% (A2), and PCM projects only slightly larger decreases of -1.1% (A2) to -1.3% (B1). At ENDCCEN, GFDL A2 and PCM B1 show decreases of -0.7% to -2%, and PCM A2 and GFDL2.1 B1 project increases of 0.2% to 0.3% (Figure 9). None of these changes are particularly significant, likely reflecting the fact that wind speed is parameterized as such a complex function of daily weather characteristics and wind direction for each location that the multiple changes in temperature, humidity, wind direction, and other factors already observed are interacting here to simultaneously increase and decrease wind speed, producing little net change. It is also likely a result of the fact that this approach does not take into account model-simulated changes in the wind-related characteristics of the daily weather systems. A comparison of these wind direction and speed projections with high-resolution regional model-generated values is planned for the future, to evaluate the ability of this approach to capture projected shifts in wind owing to climate change. However, focusing on the “very windy days” (wind speeds > 15) only, which likely display a stronger relationship to fire escapes than do the overall average wind fields for a given season, does reveal a more consistent picture of the future. For MIDCCEN, all but the GFDL A2 simulation show decreases in the number of “very windy” days (Figure 10). At ENDCCEN, however, both A2 simulations show increases of 0.2 to 0.7 windy days per season, and both B1 scenarios show decreases of 0.3 to 0.7 windy days per season. This suggests that for each model there should be a consistently larger number of wind-driven fire escapes under the A2 scenario relative to the B1 at ENDCCEN.

**Table 4. Predicted wind for the Amador-El Dorado Unit**

	<u>MEAN</u>			<u>STANDARD DEVIATION</u>		
	BASE	MIDCEN	ENDCEN	BASE	MIDCEN	ENDCEN
<b>WIND DIRECTION (ON A NORTH-INITIATED, CLOCKWISE 8-POINT DIRECTIONAL SCALE)</b>						
GFDL A2	4.86	4.90	4.95	1.55	1.55	1.54
PCM A2	4.88	4.91	4.93	1.59	1.59	1.52
GFDL B1	4.87	4.89	4.88	1.58	1.55	1.56
PCM B1	4.88	4.88	4.86	1.60	1.60	1.59
<b>WIND SPEED (MILES PER HOUR)</b>						
GFDL A2	6.28	6.30	6.24	4.04	4.06	4.06
PCM A2	6.33	6.26	6.34	4.09	4.05	4.03
GFDL B1	6.26	6.30	6.28	4.06	4.04	4.03
PCM B1	6.26	6.18	6.14	4.09	4.04	4.06
<b>VERY WINDY DAYS (WIND SPEED &gt; 15) (NUMBER OF DAYS)</b>						
GFDL A2	3.20	3.77	3.90			
PCM A2	3.93	3.77	4.10			
GFDL B1	3.90	3.63	3.23			
PCM B1	3.93	3.27	3.60			

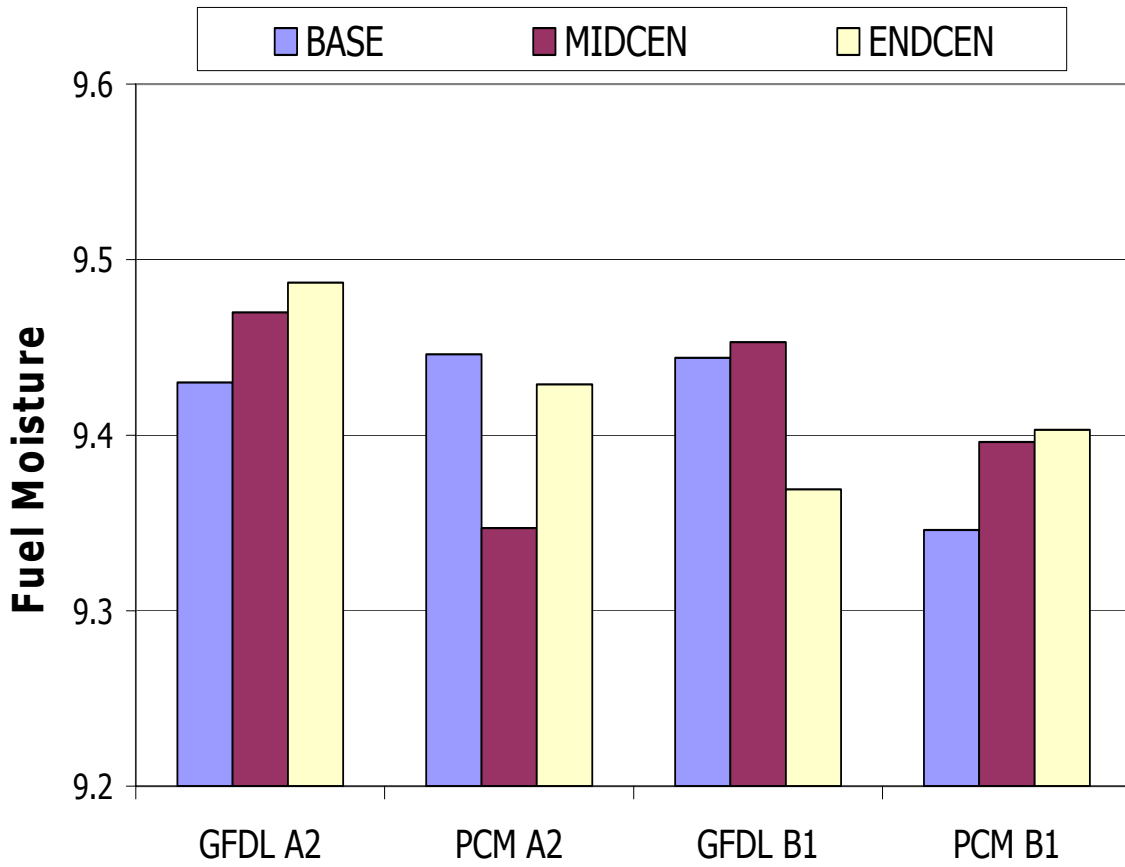


**Figure 7. Average 10-hour fuel moisture (percent) for the high and transition fire seasons, for the location of the Bald Mountain weather station, for BASE, MIDCEN, and ENDCEN, by scenario**

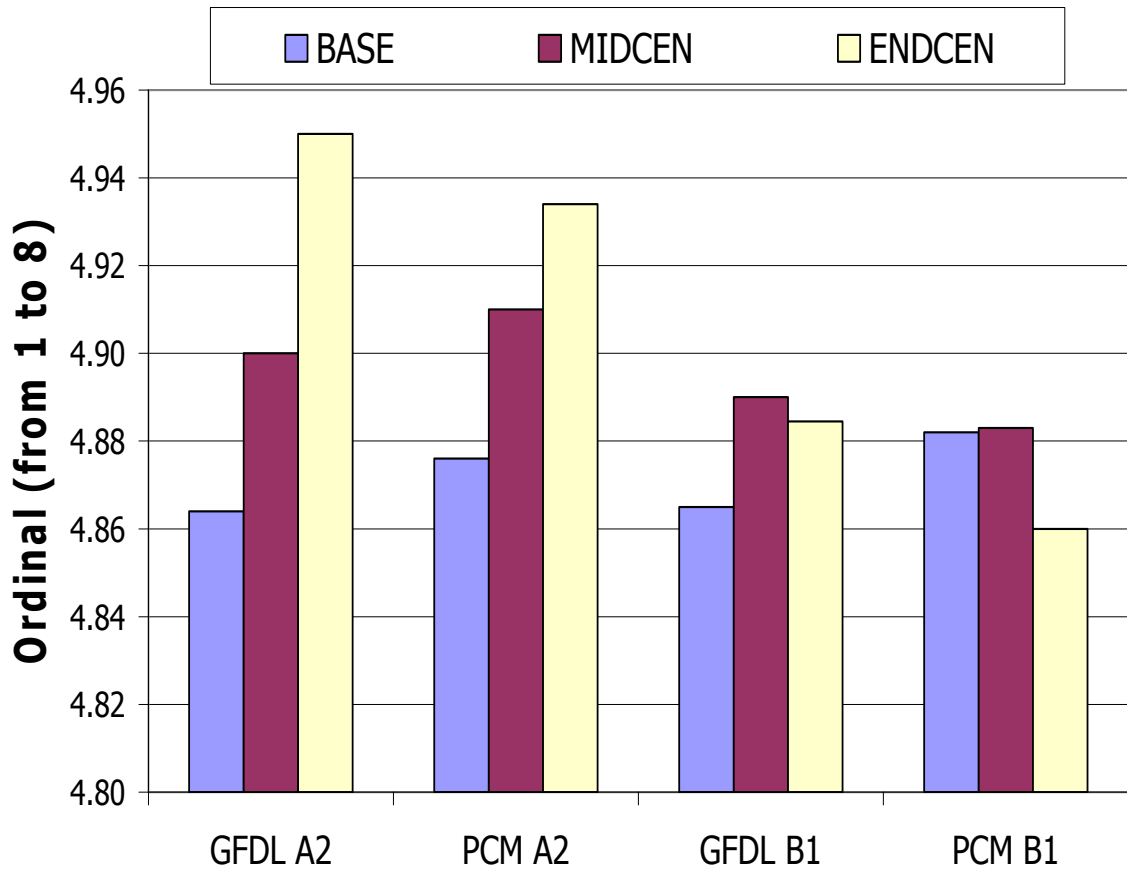


**Figure 8. Wind direction for the high and transition fire seasons, for the location of the Bald Mountain weather station, for BASE, MIDCEN, and ENDCEN, by scenario**

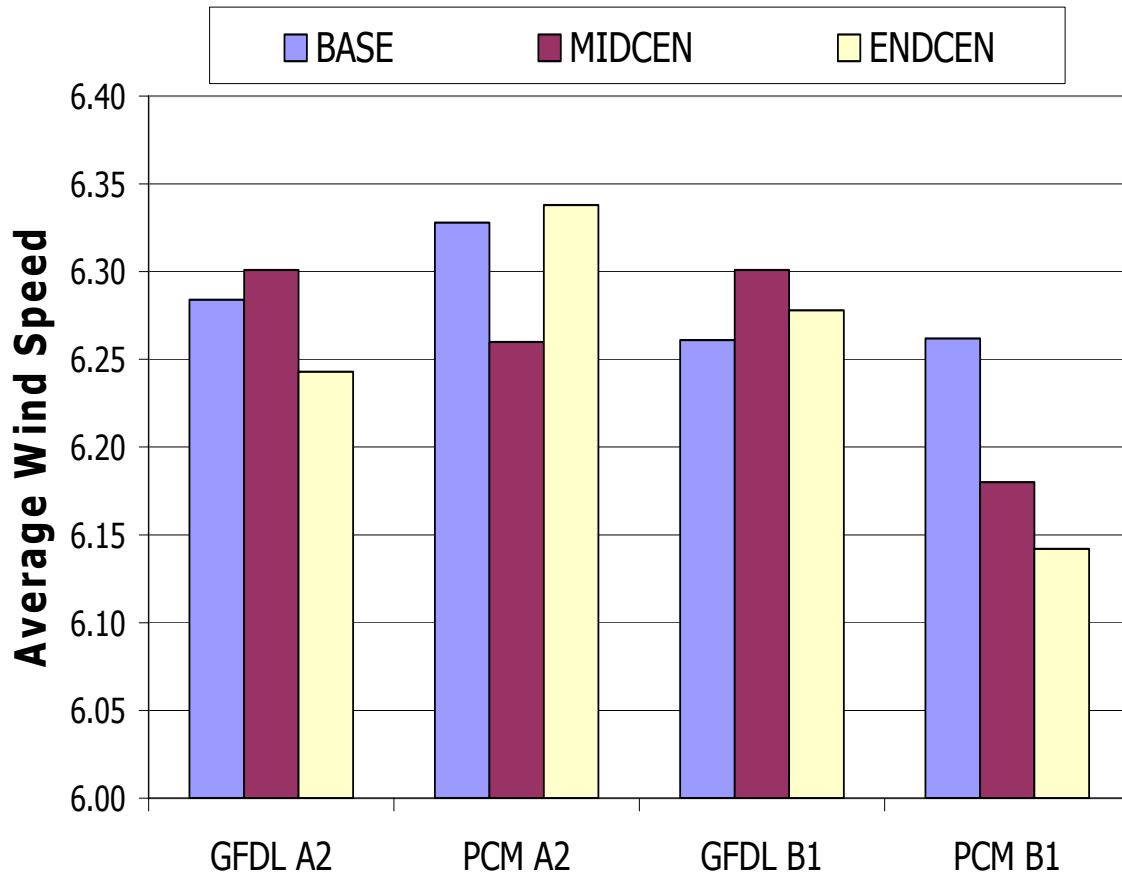


**Figure 9. Average wind speed for the high and transition fire seasons, for the location of the Bald Mountain weather station, for BASE, MIDCEN, and ENDCEN, by scenario**

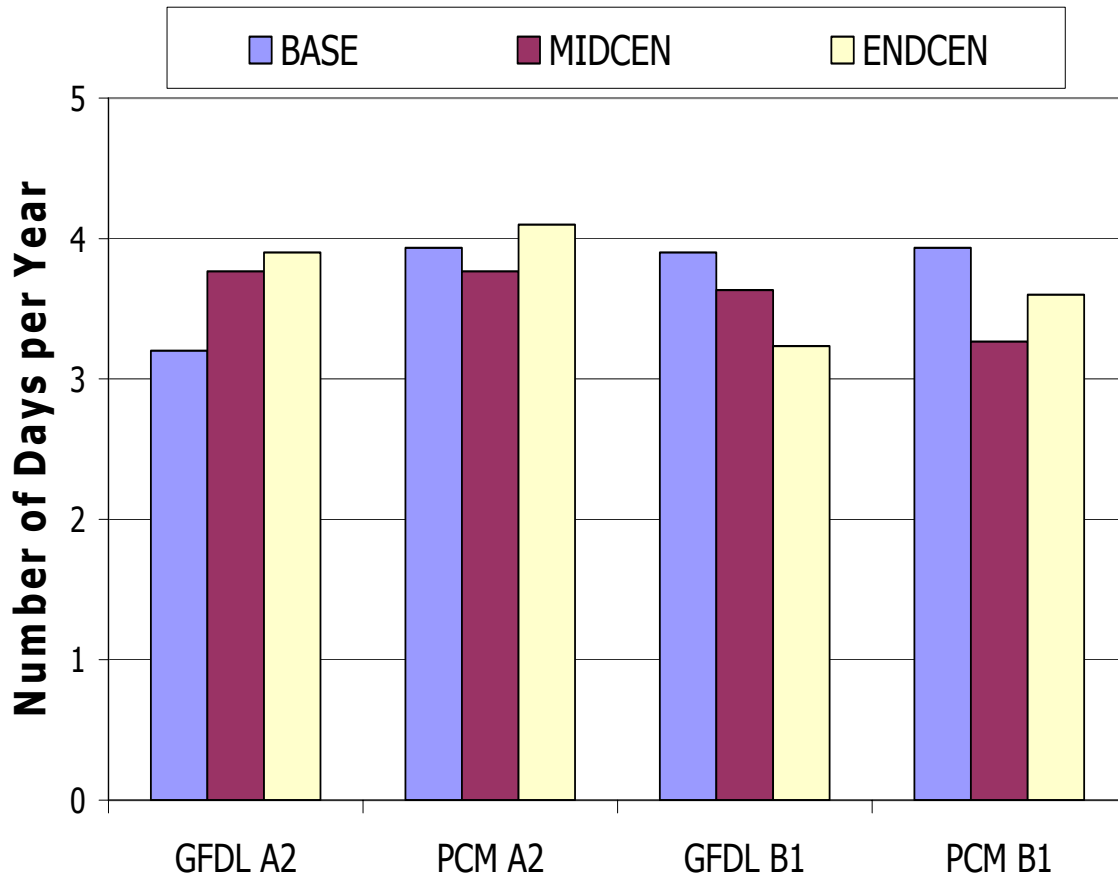


**Figure 10. Annual number of very windy days (wind speed > 15 mph) for the high and transition fire seasons, for the location of the Bald Mountain weather station, for BASE, MIDCEN, and ENDCEN, by scenario**

### 3.2. Fire Behavior

Table 5 shows mean rates of spread (ROS) for the high fire season (June 15 to October 15) under GFDL scenario A2 for selected fuel-weather station-slope class-period combinations. Note that the reported ROS means were calculated using only the portion of the distribution of predicted rate of spread values used to estimate the beta distribution that the CFES2 model uses in assigning a ROS values to faster-moving fires.

The results in Table 5 show that the increase in mean ROS between BASE and ENDCEN was significant ( $p < 0.05$ ) and positive for all fuel combinations. Relative to BASE, the largest absolute and proportional increases were for the shrub fuel combinations, and the smallest were for the timber combinations. Most of this increase, however, took place between BASE and MIDCEN, with the majority of fuel combinations showing either no change, or a slight decrease, in mean ROS between MIDCEN and ENDCEN. The exceptions were not characterized by a common fuel type. For similar fuel combinations, the predicted mean ROS was generally higher when estimated by using weather data generated for the Bald Mountain weather station (elevation 4,613 ft, or 1,406 meters) than the Georgetown weather station (elevation 3,000 ft, or 914 meters).

Table 6 shows the mean rates of spread for the same fuel combinations under the GFDL scenario A2 for just the 95th percentile values. Fires with such extremely high ROS values are of particular importance because of their greater potential to escape initial attack suppression efforts. As shown, mean ROS values for the top 5% of the estimated ROS distribution also generally increased significantly between BASE and ENDCEN for shrub and grass fuel combinations.

Table 7 shows mean ROS for the high fire season (June 15 to October 15) under GFDL scenario B1 for selected fuel-weather station-slope class-period combinations. These predicted values for mean ROS did not show as consistent a pattern of significant increase between BASE and ENDCEN for the shrub and timber fuel combinations as was evident in scenario A2. Furthermore, all fuel combinations exhibited either a decrease or no change in predicted ROS between MIDCEN and ENDCEN. These results were mirrored in Table 8, which shows the changes in predicted mean ROS for just the top 5% of the ROS distribution values.

**Table 5. Mean rates of spread (chains per hour) for the high fire season (June 15–October 15) for selected fuel-weather station-slope class-period combinations under climate model GFDL2.1, scenario A2**

Weather station	Fuel model	Slope class (percent)	Mean ROS by period			Tukey HSD comparisons		
			$\mu_{\text{BASE}}$	$\mu_{\text{MIDCEN}}$	$\mu_{\text{ENDCEN}}$	Change BASE to MIDCEN	Change MIDCEN to ENDCEN	Change BASE to ENDCEN
Bald Mountain	Grass (A1)	26–40	60.72	63.24	63.77	+	x	+
Georgetown	Grass (A1)	26–40	59.41	63.02	71.78	+	+	+
Bald Mountain	Shrub (B1)	26–40	54.10	64.53	65.09	+	x	+
Georgetown	Shrub (B1)	26–40	34.93	38.13	39.68	+	+	+
Bald Mountain	Shrub (B1)	41–55	57.34	71.21	72.06	+	x	+
Georgetown	Shrub (B1)	41–55	48.78	51.02	52.28	+	x	+
Bald Mountain	Open pine (C1)	26–40	13.92	17.20	16.49	+	-	+
Georgetown	Open pine (C1)	26–40	9.18	9.88	10.14	+	+	+
Bald Mt.	Closed pine (U1)	0–25	4.24	5.02	4.91	+	x	+
Bald Mt.	Closed pine (U1)	41–55	6.41	6.97	7.06	+	x	+

Notes:  $\mu_i$  denotes the mean rate of fire spread for the values used to estimate the beta distribution characterizing most of the fire load in period I; “+” denotes significant increase. “x” denotes no change; and “-” denotes significant decrease.

**Table 6. Mean rates of spread (chains per hour) for the high fire season (June 15–October 15) for the 95th percentile values for selected fuel-weather station-slope class combinations under climate model GFDL2.1, scenario A2**

Weather station	Fuel model	Slope class (percent)	<u>Mean ROS by period</u>			<u>Tukey HSD comparisons</u>		
			$\mu_{\text{BASE}}$	$\mu_{\text{MIDCEN}}$	$\mu_{\text{ENDCEN}}$	Change BASE to MIDCEN	Change MIDCEN to ENDCEN	Change BASE to ENDCEN
Bald Mountain	Grass (A1)	26–40	145.17	146.76	146.99	x	x	x
Georgetown	Grass (A1)	26–40	116.94	122.39	127.66	+	x	+
Bald Mountain	Shrub (B1)	26–40	88.61	95.57	94.07	+	x	+
Georgetown	Shrub (B1)	26–40	73.30	77.44	80.64	+	+	+
Bald Mountain	Shrub (B1)	41–55	99.25	106.48	105.14	+	x	+
Georgetown	Shrub (B1)	41–55	84.15	88.39	91.82	+	+	+
Bald Mountain	Open pine (C1)	26–40	23.03	24.27	23.57	x	x	x
Georgetown	Open pine (C1)	26–40	17.93	18.86	19.73	+	+	+
Bald Mountain	Closed pine (U1)	0–25	8.51	8.90	8.66	x	x	x
Bald Mountain	Closed pine (U1)	41–55	12.03	12.51	12.27	x	x	x

Notes:  $\mu_i$  denotes the mean rate of fire spread for the 95th percentile values in period I; “+” denotes significant increase; “x” denotes no change; and “–” denotes significant decrease.

**Table 7. Mean rates of spread (chains per hour) for the high fire season (June 15–October 15) for selected fuel-weather station-slope class-period combinations under climate model GFDL2.1, scenario B1**

Weather station	Fuel model	Slope class (percent)	Mean ROS by period			Tukey HSD comparisons		
			$\mu_{\text{BASE}}$	$\mu_{\text{MIDCEN}}$	$\mu_{\text{ENDCEN}}$	Change BASE to MIDCEN	Change MIDCEN to ENDCEN	Change BASE to ENDCEN
Bald Mountain	Grass (A1)	26–40	60.27	64.24	61.98	+	-	x
Georgetown	Grass (A1)	26–40	61.37	70.39	63.15	+	-	+
Bald Mountain	Shrub (B1)	26–40	62.68	55.83	50.82	-	-	-
Georgetown	Shrub (B1)	26–40	35.39	37.30	37.17	+	x	+
Bald Mountain	Shrub (B1)	41–55	69.04	58.65	55.71	-	-	-
Georgetown	Shrub (B1)	41–55	49.36	50.55	50.26	+	x	+
Bald Mountain	Open pine (C1)	26–40	15.63	13.39	12.81	-	-	-
Georgetown	Open pine (C1)	26–40	9.24	9.68	9.58	+	x	+
Bald Mountain	Closed pine (U1)	0–25	4.56	4.01	4.12	-	x	-
Bald Mountain	Closed pine (U1)	41–55	6.43	6.72	6.74	+	x	+

Notes:  $\mu_i$  denotes the mean rate of fire spread for the values used to estimate the beta distribution characterizing most of the fire load in period I; “+” denotes significant increase; “x” denotes no change; and “-” denotes significant decrease.

**Table 8. Mean rates of spread (chains per hour) for the high fire season (June 15–October 15) for the 95th percentile values for selected fuel-weather station-slope class combinations under climate model GFDL2.1, scenario B1**

Weather station	Fuel model	Slope class (percent)	Mean ROS by period			Tukey HSD comparisons		
			$\mu_{\text{BASE}}$	$\mu_{\text{MIDCEN}}$	$\mu_{\text{ENDCEN}}$	Change BASE to MIDCEN	Change MIDCEN to ENDCEN	Change BASE to ENDCEN
Bald Mountain	Grass (A1)	140.68	148.18	145.04	+	x	+	140.68
Georgetown	Grass (A1)	120.43	119.00	119.76	x	x	x	120.43
Bald Mountain	Shrub (B1)	85.62	91.85	89.21	+	x	+	85.62
Georgetown	Shrub (B1)	75.37	75.82	75.18	x	x	x	75.37
Bald Mountain	Shrub (B1)	96.30	102.73	99.82	+	x	+	96.30
Georgetown	Shrub (B1)	86.32	86.87	86.17	x	x	x	86.32
Bald Mountain	Open pine (C1)	22.08	22.96	22.95	x	x	x	22.08
Georgetown	Open pine (C1)	18.42	18.48	18.46	x	x	x	18.42
Bald Mountain	Closed pine (U1)	8.15	8.47	8.47	x	x	x	8.15
Bald Mountain	Closed pine (U1)	11.68	12.08	11.99	x	x	x	11.68

Notes:  $\mu_i$  denotes the mean rate of fire spread for the 95th-plus percentile values in period I; “+” denotes significant increase; “x” denotes no change; and “-” denotes significant decrease.

### **3.3. Initial Attack Simulation**

The two key outcomes of initial attack on wildfire that are predicted by the CFES2 model are the expected number of ESL fires (those that would exceed simulation limits on time to containment or size upon containment) and the expected area burned for all fires contained within those same limits. The ESL fires can be interpreted loosely as fires that would “escape” initial attack, since the time and size limits used to define them are primarily a reflection of what policymakers regard as an escape. In some cases, although probably not for the AEU unit for which these results were generated, these time and size limits might also be used to express bounds on what is considered a range within which the simulation process is valid (i.e., one within which topography or firefighter fatigue does not fundamentally change the nature of what is being simulated, or imply that a fire would have moved into an “extended attack” phase in which additional resources would be dispatched or firefighting tactics would need to be adjusted).

Under both the GDFL A2 and B1 scenarios, the predicted number of ESL fires and area burned by contained fires for the AEU Unit in BASE compare favorably with the historical record derived from wildland fire incidents that occurred on nonfederal lands over the period 1990 to 2000 as recorded in the Emergency Activity Reporting System maintained by CDF (Table 9). The discrepancy between BASE simulation results and the historical record was less than 20% for the number of ESL fires, and less than 30% for area burned in contained fires. The predicted distribution of the ESL fires by fuel model was also quite close to the historical record, leading us to conclude that BASE simulation results provided a good basis for both relative and absolute comparisons with the predicted wildfire outcomes for MIDCEN and ENDCEN.

Under GDFL scenario A2, ESL fires and the area burned by contained fires increased by 44% and 19%, respectively, between BASE and ENDCEN (Table 10). Under GDFL scenario B1, the increase in both was much smaller—only 10% and 8%, respectively. These differences in wildfire outcomes for the two scenarios are consistent with the climate under the A2 scenario being warmer and drier, in addition to exhibiting more “extreme wind” days, which would cause a shift in the distribution of fire rates of spread toward higher rates.

**Table 9. Historical (1990 to 2000) and GFDL (BASE) Scenario A2 escapes, ESL fires, and area burned by contained fires for the main fuel types in the Amador El Dorado Unit**

<b>Fuel type</b>	<b>Historical escapes (per year)</b>	<b>Historical area burned in contained fires (hectares per year)</b>	<b>GFDL (BASE)</b>	
			<b>ESLs (per year)</b>	<b>GFDL (BASE) area burned in contained fires (hectares per year)</b>
Brush	0.7	62.2	0.83	144
Grass	0.6	215.5	0.80	317
Interior Conifer	0.3	9.1	0.19	7
Woodland	0.4	56.3	0.07	8
Not classified	0.1	15.3	0.00	0
Overall	2.1	358.5	1.88	475

**Table 10. CFES2 predictions for the GFDL GCM and both climate scenarios**

Fuel type	Fires (per year)	ESLs (per year)						Area burned in contained fires (hectares per year)					
		BASE	SE	MIDCEN	SE	ENDCEN	SE	BASE	SE	MIDCEN	SE	ENDCEN	SE
<i>GFDL Scenario A2</i>													
Brush	204	0.83	0.05	1.36	0.06	1.32	0.07	144	3	195	3	153	5
Grass	80	0.80	0.04	0.86	0.04	1.07	0.04	317	10	351	11	363	11
Interior conifer	42	0.19	0.02	0.30	0.03	0.28	0.03	7	0	9	0	10	0
Woodland	20	0.07	0.01	0.08	0.02	0.05	0.01	8	0	10	1	12	1
Overall	346	1.88	0.07	2.59	0.08	2.72	0.09	475	10	564	11	538	12
<i>GFDL Scenario B1</i>													
Brush	204	0.86	0.05	0.80	0.05	0.87	0.06	141	3	163	3	157	3
Grass	80	0.79	0.04	0.92	0.04	0.92	0.04	317	10	351	11	339	11
Interior conifer	42	0.18	0.02	0.22	0.02	0.23	0.02	7	0	8	0	7	0
Woodland	21	0.07	0.01	0.05	0.01	0.06	0.01	10	1	11	1	10	0
Overall	346	1.88	0.07	1.99	0.07	2.08	0.08	474	10	533	11	513	11

Notes: SE denotes standard error.

Interpretation of the distribution of the increases in predicted ESL fires and acres burned in contained fires in different parts of the AEU unit is complex for a variety of reasons. For example, it is standard practice for the deployment of firefighting resources to differ by fuel, slope, and population density, with more resources deployed where fires are more difficult to contain, or where greater values are at risk. Furthermore, since CFES2 does not attempt to estimate the area burned in escaped fires, the total increase in acres burned might be significantly larger than would be indicated by the increase in estimated acres burned in contained fires for either scenario. Thus, the expected total area burned in all fires might actually go down as a result of the expected number of ESL fires going up.

In AEU, the frequency of fires in high-population-density FMAZs tends to be greater than in low-population-density FMAZs (although these results are not normalized for the total area involved), possibly reflecting the fact that most of the fires in AEU are of human origin (i.e., accidents or arson). Yet under GDFL scenario A2, the number of ESL fires increased more in the low-population-density areas between BASE and ENDCEN (Figure 11, Table 11). Under the GDFL B1 scenario, the predicted increases in both expected number of ESL fires and area burned in contained fires were still greater in low-population-density areas, but the increases were much smaller than in the GDFL A2 scenario (Figure 12).

Not surprisingly, given the smaller changes in weather variables predicted by using PCM, CFES2 simulation results for PCM-generated scenarios showed little change in ESLs or acres burned in contained fires between BASE and ENDCEN, or between the A2 and B1 scenarios (Table 12).

Another way to look at predicted changes in the number of ESL fires is to consider what happens in the worst-case years instead of expected number of ESL fires per year. Consistent with the indications in table 10 that most of the increase in the number of ESL fires would be in FMAZs with brush fuels, examination of the 95th- and 99th-percentile values for the number of ESL fires per year showed increases for both brush FMAZs between BASE and MIDCEN, but no obvious increase for FMAZs characterized by other fuel models (Table 13).

In an effort to assess what additional resources would be to offset the predicted changes in fire outcomes, a “new” fire engine was added to the preexisting configuration of firefighting resources, to be nominally dispatched from the fire station generally providing the first-responding engine to simulated wildland fires in the brush, low-population FMAZ. This addition of a single engine resulted in a reduction in the predicted number of ESL fires from 2.7 to 2.4 at ENDCEN (Table 14). Although this fell short of returning the system to the annual escape rate of 1.9 that prevailed for BASE, it is easy to envision how deployment of additional firefighting resources could achieve such a reduction.



**Table 12. CFES2 predictions for the PCM GCM and both climate scenarios**

Fuel type	Fires (per year)	ESLs (per year)						Area burned in contained fires (hectares per year)					
		BASE	SE	MIDCEN	SE	ENDCEN	SE	BASE	SE	MIDCEN	SE	ENDCEN	SE
<i>PCM, Scenario A2</i>													
Brush	206	0.78	0.05	0.84	0.05	0.95	0.05	142	3	148	3	165	3
Grass	81	0.79	0.04	0.79	0.04	0.83	0.04	339	11	315	10	344	11
Interior conifer	42	0.21	0.02	0.17	0.02	0.23	0.02	7	0	7	0	7	0
Woodland	20	0.05	0.01	0.08	0.01	0.00	0.00	9	0	9	0	0	0
Overall	348	1.82	0.07	1.87	0.07	2.00	0.07	497	11	479	10	516	11
<i>PCM, Scenario B1</i>													
Brush	208	1.00	0.05	0.88	0.05	0.82	0.05	156	3	156	3	138	3
Grass	81	0.70	0.04	0.74	0.04	0.82	0.04	313	10	332	10	337	10
Interior conifer	42	0.21	0.02	0.24	0.02	0.23	0.03	9	0	7	0	6	0
Woodland	21	0.07	0.01	0.08	0.01	0.07	0.02	8	0	10	1	8	0
Overall	352	1.97	0.07	1.94	0.07	1.93	0.07	487	10	506	11	489	11

Notes: SE denotes standard error.

**Table 13. GFDL, scenario A2, 90th and 95th percentile number of ESL fires per year**

Fuel type	Population	ESLs (per year)					
		BASE		MIDCEN		ENDCEN	
		95%	99%	95%	99%	95%	99%
Brush	High	2	2	3	3	1	3
	Low	2	3	3	4	3	4
Grass	High	1	2	1	2	1	1
	Low	2	2	2	2	2	3
	Moderate	1	2	1	2	1	2
Interior conifer	High	0	1	0	1	0	1
	Low	1	1	1	2	1	2
Woodland	High	0	1	1	1	0	1
	Low	0	1	0	0	0	1

**Table 14. Effect of adding a CDF engine at the El Dorado Hills station post-climate change under GFDL-A2**

Fuel type	Population density	ESLs		ESLs		ENDCEN with extra engine	
		BASE	SE	ENDCEN	SE	ENDCEN	SE
Brush	High	0.35	0.05	0.30	0.04	0.23	0.03
	Low	0.48	0.05	1.02	0.08	0.83	0.07
Grass	High	0.14	0.03	0.20	0.03	0.18	0.03
	Low	0.42	0.05	0.60	0.06	0.54	0.05
	Moderate	0.25	0.04	0.28	0.04	0.27	0.04
Interior conifer	High	0.03	0.01	0.02	0.01	0.03	0.01
	Low	0.17	0.03	0.27	0.04	0.29	0.04
Woodland	High	0.04	0.01	0.0	0.01	0.06	0.02
	Low	0.03	0.01	0.02	0.01	0.04	0.01
Overall		1.88		2.72		2.45	

Notes: SE denotes standard error.

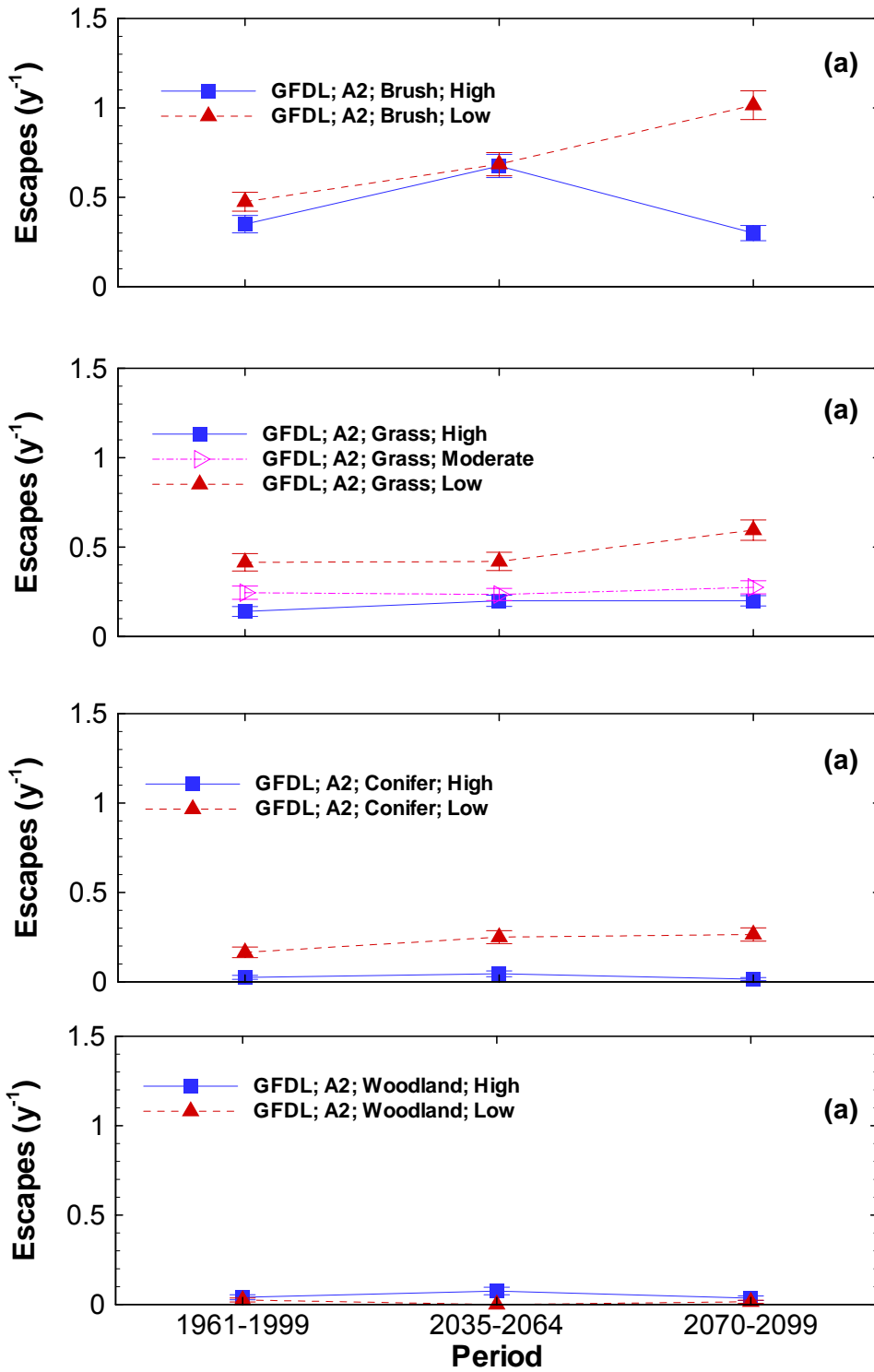


Figure 11. Mean annual escapes, by Fire Management Analysis Zone, for base, mid-century, and end-of-century periods modeled by GFDL for the A2 (high GHG) scenario

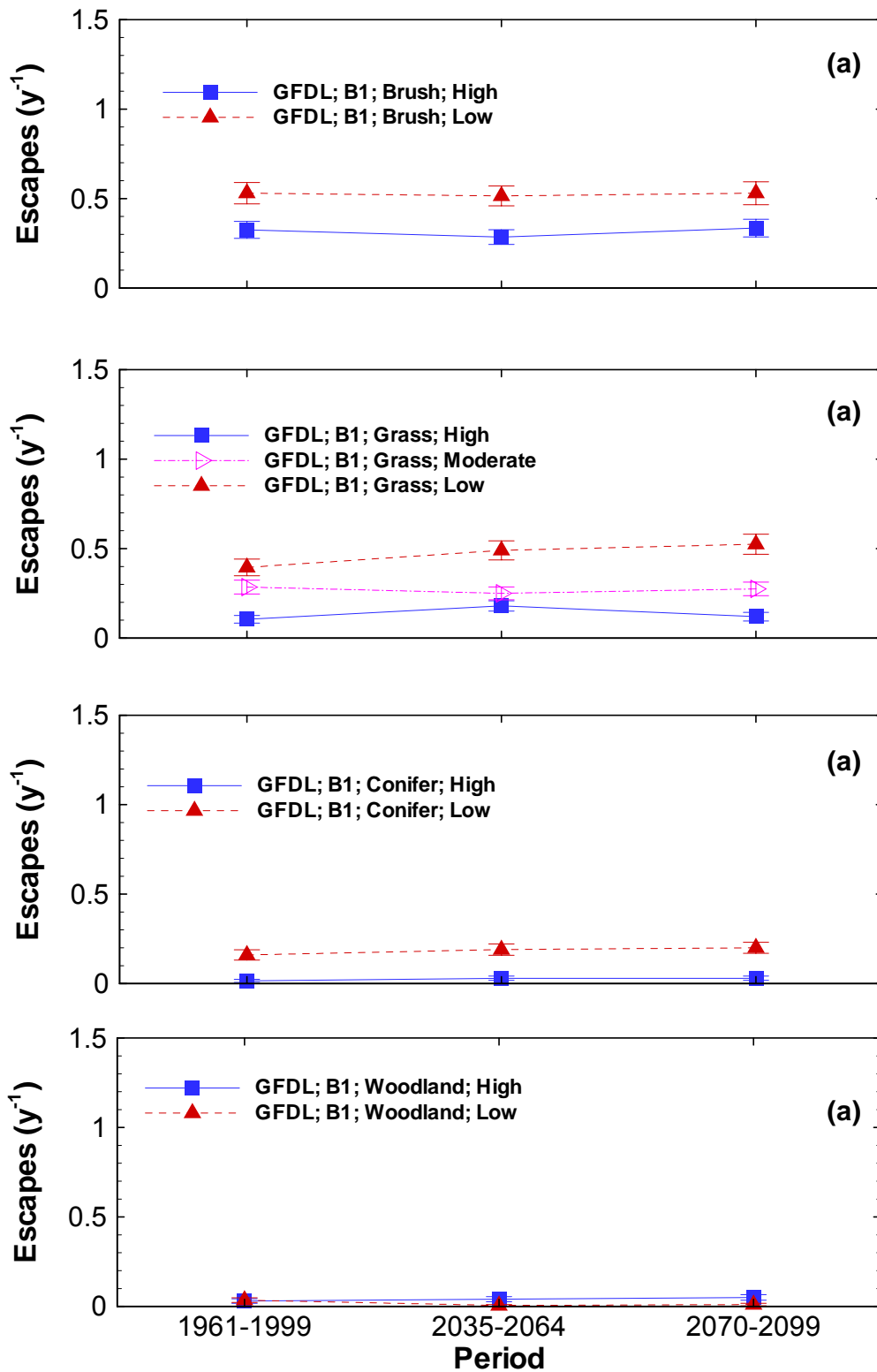


Figure 12. Mean annual escapes, by Fire Management Analysis Zone, for base, mid-century, and end-of-century periods modeled by GFDL for the B1 (reduced GHG) scenario

## 4.0 Conclusions

As climate change and population growth unfold over the coming century, we can expect changes in the wildland fire system to manifest themselves through several pathways. Climate-induced changes in weather will directly affect the behavior of vegetation fires by altering their rate of spread or intensity in ways that ultimately affect their outcomes: burned area, damage to natural resources or infrastructure, fire agency budgets and suppression expenditures, and number of fires that escape initial attack and therefore have the potential to become larger or very costly.

Just as importantly, but much more difficult to forecast, we can expect climate change to alter vegetation composition, conceivably to an extent that leads to substantial changes in the fuels available to burn, thereby affecting fire behavior. For example, if timber species die out and are replaced by shrubs, there might be less total burnable fuels and fewer commercial natural resources at risk, but fire rates of spread would likely increase.

Apart from climate change, we know that population growth will almost certainly result in additional area covered in wildland vegetation to be incorporated into California's extensive wildland-urban interface. As the wildland-urban interface spreads, the values at risk in this type of development will inexorably result in public demands for greater expenditures on firefighting resources, and for more aggressive initial attack to protect the increased values at risk. To the extent that these demands are met simply by increased use of existing resources (e.g., dispatch five engines to a fire instead of two), then this would act as a countervailing force tending to reduce any climate change-induced increase in the frequency of escaped fires without fundamentally changing the fixed costs of fire control. The effects of infrastructure development in the wildland-urban interface on the marginal costs of fire control are difficult to generalize, given their site and situation specificity.

This white paper focuses primarily on the first pathway noted above—how climate change-induced effects on weather will translate into changes in wildland fire severity and outcomes, particularly on the effectiveness of initial attack at limiting the area burned in contained fires and the number of fires that escape initial attack. The other pathways are not less important, but could not be addressed within the severe time, personnel, and resource limitations under which this work was undertaken.

Prior research on this issue indicated that there is a potential for significant increases in the number of fires escaping initial attack, particularly in areas in which the fuel matrix is dominated by grass and brush. These results were driven primarily by predicted increases in wind speeds. Those findings, however, were derived for a single climate change scenario, very coarse-scale AOGCMs, and a rather simplistic deterministic simulation model of initial attack on wildland fire (CFES-IAM).

In contrast, the analysis reported here used two state-of-the-art AOGCMs (GFDL and PCM), new downscaling techniques to link the outputs of those AOGCMs to historical data from local weather stations, and a much more sophisticated stochastic simulation model of initial attack on wildland fire (CFES2) that was developed specifically to address the deficiencies noted in the model used in the prior research on this topic. Using this more rigorous approach with data for the Amador-El Dorado Unit, this study's primary findings can be briefly summarized as follows.

First, the subtle shifts in fire behavior of the sort that might be induced by the climate changes anticipated for the next century are of sufficient magnitude to generate an appreciable increase in the number of fires that escape initial attack, at least for areas where brush fuels dominate. It is important to remember that even a fractional increase in the number of ESL fires may have significant public policy implications, given the high cost to society of a catastrophic escape like those experienced in recent decades in the Berkeley-Oakland, Santa Barbara, San Diego, or Los Angeles areas.

Second, comparison between the higher A2 and lower B1 emissions scenarios shows that the lower emissions scenario seems to be sufficient to produce modest reductions in the anticipated negative impacts on wildland fire severity and outcomes relative to the higher A2 scenario.

Third, this analysis is sensitive to the choice of AOGCM. Projections of certain climate variables that display strong relationships to fire conditions and spread (e.g., wind speed, 10-hr fuel moisture) appear to be more sensitive to the model than shown in the emissions scenario used (Tables 2, 4). Carrying these projections through to simulations of wildland fire severity, we found the PCM-generated climate scenarios (which were in general wetter than and not as warm as GFDL) to result in more modest predicted changes in wildland fire severity and outcomes than GFDL-generated climate-change scenarios. The climate impacts on fire conditions and rates of spread might be much greater in San Bernardino or Riverside, where under GFDL A2, relative humidity starts lower (compared to AEU) and declines along with precipitation, number of wet days, and precipitation intensity; whereas there are more windy days and higher wind speeds. Such changes would increase the likelihood of escapes, which highlights the importance of performing a similar analysis for a southern California CDF unit.

Fourth, the magnitude of the climate change-induced changes in wildland fire severity and outcomes was less than reported in prior work, and we suspect that this is primarily owing to different assumptions with respect to how wind speed is treated in the process of downscaling AOGCM climate simulations. The method used in this study was more conservative, sampling from historical distributions, but, lacking input from larger-scale dynamics as represented by a regional climate model, it may underestimate the effect of climate change on wind fields. Further work on how to combine the historical range of wind speeds observed at weather stations with dynamic simulations of changes in regional to local-scale wind fields under climate change scenarios and evaluation of their overall impact on wildfire severity and spread will be a high priority for the research team who collaborated to produce this report.

Fifth, we conclude that the change-induced changes in wildland fire outcomes given the existing firefighting resources, deployment, and dispatch policies in AEU could be compensated for with a modest augmentation to those resources. A modest augmentation of firefighting resources in all of the CDF's 22 administrative units and contract counties, however, might translate at the statewide level into a significant budget augmentation. As noted below, generalizing this result would be problematic until a similar analysis is performed for additional units characterized by a wider range of fuel conditions, resource availability, etc.

Sixth, although the existing "fire season" during which the CDF maintains a fully staffed organization is more a reflection of annual fire occurrence patterns than anticipated fire behavior, the results of climate change on fire behavior predicted by using the methods employed in this study suggest that fire behavior might play a more significant role in

determining the length of the fire season in the future. Further exploration of this possibility will, of course, need to be coordinated with work on how fire occurrence patterns might change as a result of both climate and demographic changes over the next century.

Seventh, it would be useful for future work to attempt to factor in vegetation change resulting from climate change, possibly by using the newer 40-fuel model system in BEHAVE 2, or perhaps the 256-fuel model matrix of the fuel characteristics classification system. The fuel models used in this study are relatively coarse, and therefore relatively unresponsive to climate change.

Eighth, although this study has focused on a consideration of the impact of climate change on rate of spread, it may be just as important to consider the impacts of climate change and vegetation management activities on the potential for crown fires. Some of the models currently in use for assessing crown fire potential would have the benefit for extension of this research of being linkable to the Forest Inventory Analysis (FIA) data on forest condition collected by the USDA Forest Service (USFS).

Finally, in contrast to prior work, the use in this study of a stochastic model of initial attack demonstrates the value of being able to generate standard errors on the mean values of predicted outcomes for hypothesis testing, as well as for characterizing the impact of climate change on the extreme values of fire ROS distributions.

Generalizing our findings with respect to wildland fire intensity and outcomes for the Amador-El Dorado Unit to other private lands in the state will require both further analysis using the AEU data, and replication of this analysis using data for several other units. We have plans to do so in the coming months, using data from the Santa Clara and San Bernardino Units.

It will be more difficult to extend the analysis to cover the public forests managed by the USFS on the north coast or in the upper elevations of the Sierra Nevada owing to differences between the USFS Fire Program Analysis (FPA) model and the California Department of Forestry and Fire Protection's CFES2 model for analysis of initial attack on wildland fires. The two models are similar in many ways, but the FPA model does not incorporate a stochastic treatment of key simulation elements (e.g., fire occurrence or rate of spread), and therefore its simulation outputs cannot be analyzed by using the same significance-testing methods. The same methods could, however, be used to downscale GCM climate projections for a similar analysis of the impact of climate change on fire rates of spread, and a deterministic analysis could be performed by using the FPA model of the effects of those changes. It is also likely that a more sophisticated analysis of the impact of climate change on wildfire on public and private lands in California would entail the development of separate prediction models of the effects on fire occurrence, as most fires on CDF-protected lands are of anthropogenic origin; whereas lightning-caused fires constitute a higher proportion of fire ignitions on much of the land protected by the USFS.

We believe that the research summarized in this paper will prove to be at least as valuable as any attempt would have been to estimate statewide impacts, if not more so, because of the problems and opportunities it has identified in our capacity to address the questions that motivated the study. In particular, it is now clear to the fire research community at the University of California, Berkeley, and to their network of collaborators at other institutions,

that much more work is needed to validate some of our modeling approaches, or develop entirely new ones, to many of the elements of the system we are modeling.

## 5.0 References

- California Department of Forestry and Fire Protection (CDF). 1992. FBDMOD: Fire behavior dispatch modeling system. Sacramento, California.
- Davis, F. W., and J. Michaelsen. 1995. Sensitivity of fire regime in chaparral ecosystems to global climate change. In: Moreno, J.M., Oechel, W.C. (Eds) *Global Change and Mediterranean-Type Ecosystems*. Springer-Verlag, New York, 435–456.
- Deeming, J. E., R. E. Burgan, and J. D. Cohen. 1977. The National Fire Danger Rating System 1978, General Technical Report INT-39, USDA Forest Service Intermountain Forest and Range Experiment Station, 63 pp.
- Delworth, T. L., A. J. Broccoli, A. Rosati, R. J. Stouffer, et al. 2005. “GFDL’s CM2 global coupled climate models–Part 1–Formulation and simulation characteristics.” *J. Clim.*, in press.
- Fried, J. S., and J. K. Gilless. 1988. Stochastic Representation of Fire Occurrence in a Wildland Fire Protection Model for California. *Forest Science* 34:948–955.
- Fried, J. S., and J. K. Gilless. 1999. *CFES2: The California Fire Economics Simulator Version 2 User’s Guide*, University of California, Division of Agriculture and Natural Resources Publication 21580, 92 pp.
- Fried, J. S., J. K. Gilless, and J. Spero. 2006. “Analysing initial attack on wildland fires using stochastic simulation.” *International Journal of Wildland Fire* (In Press)
- Fried, J. S., M. S. Torn, and E. Mills. 2004. “The impact of climate change on wildfire severity: A regional forecast for Northern California. *Climatic Change* 64:169–191.
- Gilless, J. K., and J. S. Fried. 1999. “Stochastic representation of Fire Behavior in a Wildland Fire Protection Planning Model for California.” *Forest Science* 45:492–499.
- Nakićenović, N., J. Alcamo, G. Davis, B. de Vries, J. Fenhann, S. Gaffin, K. Gregory, A. Grübler, T. Y. Jung, T. Kram, et al. 2000. *IPCC Special Report on Emissions Scenarios*. Cambridge University Press, Cambridge, United Kingdom and New York, New York.
- National Wildfire Coordinating Group (NWCG). 2002. *Gaining and Understanding of the National Fire Danger Rating System*. Publication PMS 932, NFES 2665.
- Torn, M. S., and J. S. Fried. 1992. “Predicting the impacts of global warming on wildland fire.” *Climatic Change* 21(3):257–274.
- Van Rheezen, N. T., A. W. Wood, R. N. Palmer, and D. P. Lettenmaier. 2004. “Potential implications of PCM climate change scenarios for California hydrology and water resources.” *Climatic Change* 62:257–281.
- Washington, W. M., J. W. Weatherly, G. A. Meehl, A. J. Semtner, T. W. Bettge, A. P. Craig, W. G. Strand, J. Arblaster, V. B. Wayland, R. James, and Y. Zhang. 2000. “Parallel climate model (PCM) control and transient simulations.” *Climate Dynamics* 16:755–774.
- Wood, A. W., L. R. Leung, V. Sridhar, and D. P. Lettenmaier. 2004. “Hydrologic implications of dynamical and statistical approaches to downscaling climate model outputs.” *Climatic Change* 62:189–216.

Wood, A. W., E. P. Maurer, A. Kumar, and D. P. Lettenmaier. 2002. "Long range experimental hydrologic forecasting for the eastern U.S." *J. Geophys. Res.* 107(D20), 4429.